



Evaluating the Impact of Tidal Energy in the Cook Inlet on Alaska's Railbelt Electrical Grid

Marty Schwarz, Ben McGilton, Levi Kilcher, Kelly Gjestvang, and Greg Stark

National Renewable Energy Laboratory

**NREL is a national laboratory of the U.S. Department of Energy
Office of Energy Efficiency & Renewable Energy
Operated by the Alliance for Sustainable Energy, LLC**

This report is available at no cost from the National Renewable Energy Laboratory (NREL) at www.nrel.gov/publications.

Contract No. DE-AC36-08GO28308

Technical Report
NREL/TP-5700-85943
April 2024



Evaluating the Impact of Tidal Energy in the Cook Inlet on Alaska's Railbelt Electrical Grid

Marty Schwarz, Ben McGilton, Levi Kilcher, Kelly
Gjestvang, and Greg Stark

National Renewable Energy Laboratory

Suggested Citation

Schwarz, Marty, Ben McGilton, Levi Kilcher, Kelly Gjestvang, and Greg Stark. 2024.
*Evaluating the Impact of Tidal Energy in the Cook Inlet on Alaska's Railbelt Electrical
Grid*. Golden, CO: National Renewable Energy Laboratory. NREL/TP-5700-85943.
<https://www.nrel.gov/docs/fy24osti/85943.pdf>.

**NREL is a national laboratory of the U.S. Department of Energy
Office of Energy Efficiency & Renewable Energy
Operated by the Alliance for Sustainable Energy, LLC**

This report is available at no cost from the National Renewable Energy
Laboratory (NREL) at www.nrel.gov/publications.

Contract No. DE-AC36-08GO28308

Technical Report
NREL/TP-5700-85943
April 2024

National Renewable Energy Laboratory
15013 Denver West Parkway
Golden, CO 80401
303-275-3000 • www.nrel.gov

NOTICE

This work was authored by the National Renewable Energy Laboratory, operated by Alliance for Sustainable Energy, LLC, for the U.S. Department of Energy (DOE) under Contract No. DE-AC36-08GO28308. Funding provided by U.S. Department of Energy Office of Energy Efficiency and Renewable Energy Water Power Technologies Office. The views expressed herein do not necessarily represent the views of the DOE or the U.S. Government.

This report is available at no cost from the National Renewable Energy Laboratory (NREL) at www.nrel.gov/publications.

U.S. Department of Energy (DOE) reports produced after 1991 and a growing number of pre-1991 documents are available free via www.OSTI.gov.

Cover Photos by Dennis Schroeder: (clockwise, left to right) NREL 51934, NREL 45897, NREL 42160, NREL 45891, NREL 48097, NREL 46526.

NREL prints on paper that contains recycled content.

Acknowledgments

The authors would like to thank Homer Electric Association for their assistance with the development of the Alaska Railbelt production cost model and for supporting this investigation and report. The authors also thank the U.S. Department of Energy's Water Power Technologies Office for their support of this analysis and report.

The authors would also like to thank the following individuals from the National Renewable Energy Laboratory: Katie Peterson, David Palchak, Tessa Greco, and Mike Lawson for their helpful review and comments; Billy J. Roberts for generating the maps; and Amy Brice for editing.

List of Acronyms

AEP	annual energy production
BESS	battery energy storage system
CH ₄	methane
CO ₂	carbon dioxide
DOE	U.S. Department of Energy
EPA	U.S. Environmental Protection Agency
GVEA	Golden Valley Electric Association
GWh	gigawatt-hour
HEA	Homer Electric Association
kV	kilovolt
kWh	kilowatt-hour
m/s	meters per second
mg/L	milligrams per liter
MW	megawatt
N ₂ O	nitrous oxide
NOAA	National Oceanic and Atmospheric Administration
NREL	National Renewable Energy Laboratory
PV	photovoltaic
TWh/yr	terawatt-hours per year
Tx	thermal rating

Executive Summary

This report presents the findings of a case study that evaluates the impact of integrating significant tidal energy generation in the Cook Inlet in Alaska. The case study is part of a series within the “Quantifying the Grid Value of MRE [Marine Renewable Energy] in Early U.S. Markets” project funded by the U.S. Department of Energy (DOE).¹

The Cook Inlet represents approximately 30% of the total tidal energy in the United States. It is located alongside the Kenai Peninsula, a region serviced by the Homer Electric Association (HEA). HEA constitutes the southernmost portion of Alaska’s Railbelt electricity grid, which in its entirety serves approximately 75% of the state’s population and stretches across southcentral Alaska from Homer in the south to Fairbanks in the north. The Railbelt utilities sold 4,408 gigawatt-hours (GWh) of electricity in 2020, and HEA’s sales were 11% of that (496 GWh). Despite significant natural resources, Alaska is among the states with the highest energy prices. Increasing renewable energy in the region has been proposed to address these high prices. Because of the substantial and highly predictable tidal flow rate in the inlet, along with its proximity to the majority of Alaska’s population, tidal energy generation has been proposed; however, there have been no studies to date that evaluate its potential as part of a mixed energy portfolio from a grid integration perspective.

This study takes a scenario-based approach to evaluate the tidal energy potential in the Cook Inlet, in which 100–500 megawatts (MW) of tidal energy are integrated into the grid under different infrastructure scenarios. These scenarios include increased energy storage and transmission line upgrades, a “Basecase” scenario with no additional upgrades, and a reference case with no tidal energy.

The project team worked with HEA to develop a model of the entire Railbelt grid in the price-maker production cost modeling software PLEXOS by Energy Exemplar.² The final model closely aligns with the utility’s models. The model simulates 2035 by scaling load and adding new wind, solar photovoltaic (PV), and battery storage plants already undergoing feasibility studies. Table ES-1 lists the plants included at the time of modeling in November 2022. Because of scheduling and review conflicts associated with the DOE Funding Opportunity Announcement for U.S. Tidal Energy Advancement (DE-FOA-0002845), the publication of this report was delayed, and some of these assumptions may require updating in any subsequent modeling and analysis.

¹ As a first-of-its-kind case-study for the challenges and opportunities of tidal energy in a utility-scale power system, this work is not an engineering study or a detailed financial feasibility analysis. Its purpose is to identify the upper limit of value, from a production cost modeling perspective, that tidal energy could supply to the Railbelt power system. It simplifies the Railbelt system into a three-zone model, ignores existing contractual obligations, and does not capture tidal capital costs or electrical engineering integration challenges beyond energy balancing. A complete interconnection study would need to be completed before the tidal energy could be safely integrated to the Railbelt system.

² <https://energyexemplar.com/solutions/plexos/>

Table ES-1. List of Planned New Renewable Energy and Storage Projects

Plant name	Technology	Capacity	Location
Delta Wind Farm	Wind	90 MW (currently 1.9 MW)	Golden Valley Electric Association (GVEA)
Eva Creek Wind Farm	Wind	25 MW	GVEA
HEA Wind Farm 1	Wind	31 MW	HEA
Nenana Solar	Solar utility PV	16 MW	GVEA
Homer Utility Solar	Solar utility PV	30 MW	HEA
Homer Residential Solar	Solar distributed PV	3 MW	HEA
Chugach Battery Energy Storage System (BESS)	Battery storage	70 MW, 4-hour	Central
GVEA BESS	Battery storage	100 MW, 2-hour	GVEA
HEA BESS	Battery storage	46 MW, 2-hour	HEA

The tidal energy generation was modeled with actual tidal flow rate data obtained from the National Oceanic and Atmospheric Administration current meter stations and extrapolated for extended time periods with a representative tidal energy converter power curve. This analysis and the key findings should be viewed as a starting point for additional research and used to inform investment and policy options. There are three key findings from the work:

Key Finding 1: While the reported theoretical tidal resource is greater than 18,000 MW in the inlet, this study found that the existing electrical transmission constraints along the Kenai Intertie impose a practical limit of approximately 200 MW on installed capacity. Potential transmission upgrades may extend this limit to nearly 185 MW, but capacity expansion beyond that would require either (1) additional transmission upgrades or (2) additional dispatchable load near the site of the tidal generation.

Key Finding 2: By doubling the rating of the Kenai Intertie, tidal energy could contribute up to 25% of the total Railbelt electrical load, reduce annual carbon dioxide emissions by more than 29%, and lower annual fuel cost by more than 16% without significant curtailment.

Key Finding 3: By distributing the tidal array along the inlet and capitalizing on the fact that the tidal currents peak at different times along the inlet, it is possible to increase the capacity of tidal energy that the grid could handle without major transmission upgrades.

With these findings, we concluded that tidal energy at an installed capacity of 200–300 MW has the potential to reduce fuel costs in Alaska while also reducing carbon emissions and increasing the energy independence of the state.

Caveats:

While this study simulates the hourly unit commitment and economic dispatch of every power plant and both high-voltage transmission lines in the Railbelt power system, it is not a prediction for the realistic hourly operation of the Railbelt in a future year. The findings in this paper should be considered with the following caveats in mind:

- This study does not attempt to predict an accurate power system infrastructure in 2035.
- Tidal energy technology is a precommercial technology.
- This is an idealized view of Railbelt operation.
- We do not model the complex power purchase agreements that would be required to absorb all the non-curtailed tidal energy.
- We assume that tidal energy could take priority on the Kenai Intertie.

The purpose of this study was to identify whether tidal energy could be an opportunity for the Railbelt, and the results show that tidal energy could supply a significant portion of the Railbelt's electrical demand. However, much more analysis is needed before actual tidal energy integration could take place, such as detailed engineering studies that investigate sub-second dynamic response of the new technology, interconnection studies, financial feasibility studies, and more.

Table of Contents

Executive Summary	v
1 Introduction	1
2 Methodology	6
2.1 Basecase Formulation	6
2.2 Tidal Energy Data	7
2.3 Tidal Power Model	8
3 Scenario Outline, Results, and Analysis	10
4 Results	12
4.1 Total Generation	12
4.2 Curtailment	14
4.3 Impact of Tidal Energy on Systemwide Generation Cost	16
4.4 Impact of Tidal Energy on Thermal Power Plant Emissions	19
4.5 Impact of Tidal Energy on Transmission Utilization	20
5 Investigation of Tidal Array Placement Along the Cook Inlet	24
6 Summary and Conclusion	28
References	29
Appendix A. Device and Array Sizing	31
Appendix B. Full Set of Generation Results	35

List of Figures

Figure 1. Map of Alaska's Railbelt power system with four service territories: Golden Valley Electric Association, Matanuska Electric Association, Chugach Electric Association, and Homer Electric Association.	2
Figure 2. Total generation capacity, by region, for the Basecase system in 2035	7
Figure 3. A comparison of measurements from NREL's 2021 resource characterization project (green) with a tidal harmonic fit to that data (black) for East Foreland, and an extrapolation of a harmonic fit to data collected by NOAA at a nearby site in 2005	8
Figure 4. Total annual generation stacks for a representative subset of scenarios. The full set of total generation results can be found in Appendix B.	12
Figure 5. Total annual generation stacks for a representative subset of scenarios, compared to the Basecase infrastructure with no tidal energy capacity. The full set can be found in the Appendix.	13
Figure 6. Total annual tidal energy curtailment as a function of both installed capacity and infrastructure upgrade scenario. The black dashed line represents 5% curtailment. Note the "Tx" values are almost identical to the "Tx-BESS" values.	15
Figure 7. Total systemwide fuel cost, as a function of installed tidal capacity and infrastructure upgrade scenario. The black dashed line shows the cost with no tidal energy deployment.	16
Figure 8. Total systemwide fuel cost as a function of total tidal energy injected (i.e., tidal energy that was not curtailed). The oval highlights the impact of various infrastructure upgrades on fuel cost reduction, while keeping the total tidal energy injected constant. Upgrading the Kenai Intertie has the largest impact on fuel cost reduction.	17
Figure 9. Similar to Figure 7, but showing the fuel cost savings from the no-infrastructure-upgrades Basecase. The x-axis shows tidal energy deployment, rather than tidal energy injection.....	18
Figure 10. Total systemwide startup and shutdown costs (also referred to as cycling costs) as a function of tidal energy injected and infrastructure upgrade scenario for 2035 infrastructure with no new wind or solar PV. The black dashed line shows the value for the scenario with no tidal energy. Consistent with other metrics, the copperplate scenarios have the highest impact on this cost category. However, the impact is an order of magnitude smaller than that for fuel cost.	19
Figure 11. Total power plant emissions under each tidal energy and infrastructure upgrade scenario. As before, the black dashed line represents the value in a system with no tidal energy. From left to right, the panels show CO ₂ , CH ₄ , and N ₂ O emissions. The y-axis lower limit of zero is removed to increase clarity.	20
Figure 12. Flow duration curves for the Kenai Intertie in the 150-MW tidal deployment scenarios. Note the "Tx" values (purple) are almost identical to the "Tx-BESS" values (red). Additionally, the "BESS" values (green) are almost identical to the "Basecase" values (blue).	21
Figure 13. Similar to Figure 12, but showing flow duration curves for all tidal capacity scenarios	22
Figure 14. Map showing four theoretical locations for tidal energy throughout the Cook Inlet.....	25
Figure 15. Tidal current speed profiles (upper panel) for the three southern Cook Inlet sites. The phase difference in tidal cycles means that the combined power output from the three sites (lower panel) is never zero. In this case, each site has 33 MW of capacity, for a total of 99 MW. ...	25
Figure 16. Total annual tidal energy curtailment with capacity all placed at each of the three southern Cook Inlet sites, and an even split between the three sites. The flat black dashed line represents 5% curtailment. Above this number, the curtailment technology may lose economic viability.	26
Figure 17. Correlogram between tidal energy profiles for all four sites studied and total Railbelt-wide net load. The Kennedy Entrance site is the most negatively correlated with the other sites. It is also the site most negatively correlated with net load, though this value is near-negligible. ...	27

Figure A-1. The generator power curve (right axis), and probability density function (pdf) of ocean velocity at the East Foreland (bars, left axis). The power curve is plotted for three different generator sizes, with three different capacity factors..... 32

Figure A-2. Total power captured at the East Foreland site for a single device (left, blue axis), the capacity factor for the device (right, red axis), and U_{rated} versus generator capacity (P_{rated}). The square and triangle markers indicate the AEP and capacity factor, respectively, for the generator sizes in Figure A-1. Dotted lines indicate the values for sizing the generator to capture 95% of the power available to the rotor. In this case, 95% of the maximum AEP can be captured with a 1.17-MW generator..... 33

Figure A-3. Array layout diagram in plan view (i.e., from above looking down) 34

Figure B-1. Total generation stacks for all scenarios studied. Results plotted are Railbelt-wide..... 35

Figure B-2. Total generation stacks, differenced from the Basecase with no tidal energy, for all scenarios studied. Results plotted are Railbelt-wide..... 35

List of Tables

Table ES-1. List of Planned New Renewable Energy and Storage Projects..... vi

Table 1. List of Planned New Renewable Energy and Storage Projects..... 7

Table 2. Tidal Turbine Device and Array Sizing for Several Sites in Cook Inlet 9

Table 3. Scenario Description..... 11

Table 4. Emissions Rates for Different Thermal Power Plant Technologies in Alaska 20

1 Introduction

Despite its wealth of energy resources, both renewable and conventional, Alaska is among the states with the highest energy prices. In Alaska's Railbelt electricity grid—which serves approximately 75% of the state's population and stretches across southcentral Alaska from Homer in the south to Fairbanks in the north (Figure 1)—residential rates are as high as \$0.25 per kilowatt-hour (kWh). Rural Alaska energy prices are the highest in the nation, often more than \$1/kWh. These high prices create attractive market conditions for emerging energy technologies, such as tidal energy, whose costs are currently too high and uncertain to compete in lower-price markets. Furthermore, declining natural gas supplies in Cook Inlet and declining North Slope oil production are forcing the state to reassess its long-term energy strategies for both domestic use and export (DeMarban 2022; Marohl 2021; Alyeska Pipeline 2023).

Approximately one-third of the nation's tidal energy resource is estimated to be in Alaska's Cook Inlet, and more than 90% of the nation's tidal resource is distributed throughout Alaska (Kilcher, Fogarty, and Lawson 2021). The technical resource potential of Cook Inlet is estimated to be 80 terawatt-hours per year (TWh/yr)—more than 15 times the present-day Railbelt electricity consumption of approximately 5.2 TWh/yr (U.S. Energy Information Administration 2023). The most promising tidal energy sites in Cook Inlet are located alongside the Kenai Peninsula, where Homer Electric Association (HEA) operates the southernmost portion of Alaska's Railbelt electricity grid. HEA has a customer base of approximately 33,000 customers and sold 496 gigawatt-hours (GWh) of power in 2020—with an average load of approximately 56 megawatts (MW) (HEA 2020). As the sole grid operator south of the Kenai Intertie, HEA has a unique stake in and responsibility for the integration of tidal energy into the Railbelt grid. Furthermore, HEA plays a critical role in the Railbelt grid as the operator of the Bradley Lake hydroelectric facility—the largest hydroelectric power station in the state (Homer Electric Association Inc. n.d.).

Tidal energy provides unique opportunities to the HEA system and Railbelt grid. In particular, the channel just offshore of the East Foreland, near Nikiski Alaska, contains high quality tidal energy resources near the transmission network (see Figure 14 for a map of the Cook Inlet with the East Foreland identified). An existing high-voltage substation located near the project site could be used to interconnect tidal energy to the HEA system. Additionally, unlike most renewables, tidal energy is highly predictable and has the potential to provide baseload when combined with energy storage.

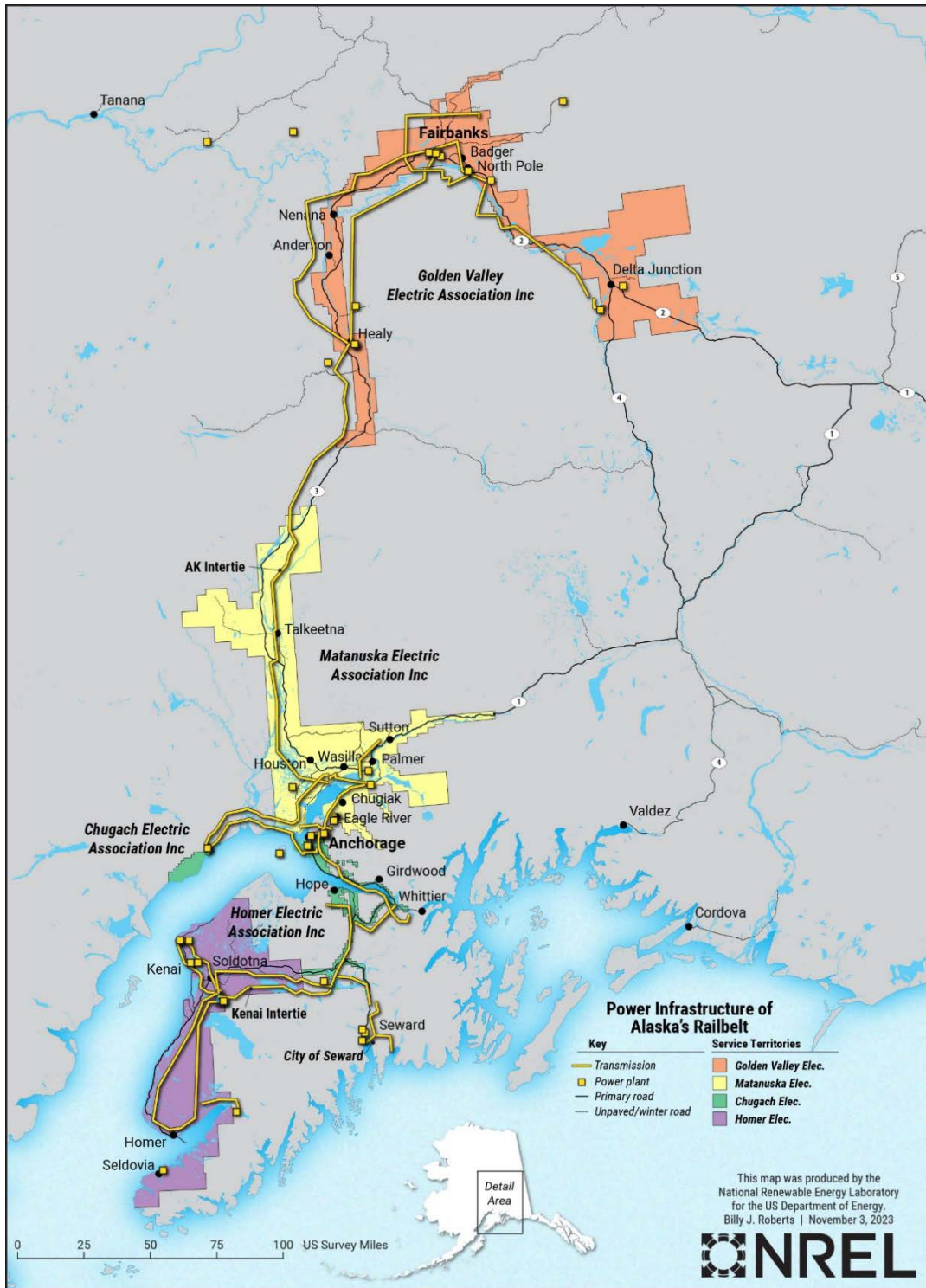


Figure 1. Map of Alaska's Railbelt power system with four service territories: Golden Valley Electric Association, Matanuska Electric Association, Chugach Electric Association, and Homer Electric Association.

Map by Billy J. Roberts, NREL

Despite the clear advantages and economic potential, relatively little research is available to support tidal energy integration in Alaska. This work seeks to address the knowledge gaps regarding the impacts of marine renewable energy to grids by modeling large capacities of tidal energy in a detailed production cost model, using the Alaskan Railbelt power system as a case study. The output of this work is designed to be useful for both tidal energy and marine renewable energy developers when scoping and proposing potential projects, and for utility stakeholders when considering proposals and planning future investment and grid operation strategies.

In late 2021, researchers at the National Renewable Energy Laboratory (NREL) collected velocity, turbulence, and sediment measurements at the East Foreland site. These data show that the East Foreland has (1) the potential for at least 100 MW of tidal energy capacity, (2) peak currents of more than 3 meters per second (m/s), and (3) sediment concentrations exceeding 200 milligrams per liter (mg/L). Data from these measurements are available on the Marine and Hydrokinetic Data Repository (Kilcher and McVey 2021). There are very few U.S. sites outside of Alaska capable of supporting projects of this scale, and the sites that could support these projects have much slower tidal current speeds. Other energetic sites within Alaska are located much farther from the transmission grid.

Denholm et al. (2022) conducted the first known production cost study of the entire Railbelt system. In that work, researchers investigated the costs and operational impacts of serving 80% of Railbelt-wide electrical load with renewable sources by 2040. They analyzed five different portfolios of electricity generation technologies, which included various new builds of wind, solar, hydropower (conventional dam storage and run-of-river), geothermal, biomass, landfill gas, and tidal energy. In two of the five scenarios, tidal energy served 3% and 5% of the total electrical demand.

Building on that previous study, this report investigates the impact of integrating new tidal energy plants in the Cook Inlet in the year 2035. However, rather than model various mixes of renewable energy in the future Railbelt grid, our analysis focuses solely on tidal energy. To this end, we only include new wind and solar photovoltaic (PV) builds associated with likely projects, such as a 90-MW wind plant in the Fairbanks region. Refer to Table 1 in the next section for the full list of planned new renewable energy and storage projects included in the model. The analysis was performed with the leading market simulation platform PLEXOS,³ which is used by HEA and other regional utilities in energy portfolio planning. Through a subcontract with HEA, the project team was able to develop a PLEXOS model of the Railbelt that directly aligns with utility models. While this alignment allows for a high-fidelity analysis, it is not necessarily meant to represent a realistic build-out of the Railbelt system; rather, it is an exploratory study designed to elucidate the limits of tidal energy contribution to the electrical demands of the Railbelt power system.

With a number of full-scale deployments, tidal energy systems have reached a high technology readiness level and precommercial status. This work is intended to evaluate the technology from

³ <https://energyexemplar.com/solutions/plexos/>

a grid integration perspective and be a starting point for additional research and consideration of investment or policy options.

Caveats:

As a first-of-its-kind case-study for the opportunities and challenges of tidal energy in a utility-scale power system, this work is not an engineering study or a detailed financial feasibility analysis. Its purpose is to identify the upper limit of value that tidal energy could supply to the Railbelt power system. While this study simulates the hourly unit commitment and economic dispatch of every power plant and both high-voltage transmission lines in the Railbelt power system, it is not a prediction for the realistic hourly operation of the Railbelt in a future year. The findings in this paper should be considered with the following caveats in mind:

- *This study does not attempt to predict a least-cost power system infrastructure in 2035.* In particular, it does not determine the cost-optimal build-out based on a holistic comparison of cost projections for all electricity generation technologies (for such an analysis, see Denholm, Schwarz, and Streitmatter [2024]). Rather, this work represents an upper limit for the opportunities for tidal energy on the Railbelt power system, assuming no other technologies are deployed beyond those already in the pipeline.
- *This study assumes megawatt-scale tidal energy will be available in large quantities by 2035.* Tidal energy technology is still in its nascency. The hourly power production profiles used to model tidal energy in this study are based on the best available understanding of the power conversion technology and direct measurements of the tidal resource in the Cook Inlet. However, tidal power plants of the scale modeled in this paper have not yet been built, and the supply chain required to build them in Alaska has not yet been developed. Our choice to model the Railbelt in 2035 relies on the assumption that such a supply chain will be developed by then.
- *This is an idealized view of Railbelt operation.* At present, each utility within the Railbelt power system (Homer Electric Association, Chugach Electric Association, Golden Valley Electric Association, Matanuska Electric Association, and the City of Seward municipal utility) operates relatively independently. This means that electricity may not always be freely traded between service regions, the utilities procure their own reserves, and power from Bradley Lake is contractually divided between utilities. By contrast, this study assumes the entire Railbelt operates as a single balancing area. While we still procure reserves separately for each of the three zones, we do not enforce any contractual obligations surrounding the partitioning of power from Bradley Lake, flow along either the Alaska or Kenai interties, or the cost of renewable energy curtailment, which refers to extra available renewable energy that could not be injected into the grid due to transmission constraints or insufficient demand, within current power purchase agreements. There is interest among the utilities to move closer to such an operational paradigm, and we assume that by 2035 existing contractual arrangements could be amended to allow for more coordinated and flexible systemwide operations.
- *We do not model the complex power purchase agreements that would be required to absorb all the non-curtailed tidal energy.* At the higher capacities we modeled, HEA

would not be able to absorb all the tidal energy, so other utilities would be required to buy it. We assume that the Railbelt will operate in such a manner that minimizes the total systemwide cost, rather than each utility independently maximizing revenue. In general, NREL's integration studies do not model power purchase agreements for any electrical generation technology.

- *We assume that tidal energy could take priority on the Kenai Intertie.* Cost-optimal systemwide operation means the cheapest energy source on the Railbelt will serve load anywhere in the system. This means that the transmission system—particularly the Kenai Intertie—will operate in any physically feasible manner necessary to transport cheap energy to load centers. In reality, however, the transmission lines are strictly partitioned; for instance, the Kenai Intertie currently exports more than 372 GWh per year from Bradley Lake hydropower to the Anchorage region. This leaves little room for tidal energy exports. We assume that the contracts denoting such operation of the Kenai Intertie and Bradley Lake power partitioning could be amended by 2035 to accommodate the influx of cheap tidal energy. However, this study is not meant to evaluate the detailed financial arrangements that would be required to integrate significant portions of tidal energy on the Railbelt power system.

The purpose of this study was to identify whether tidal could be an opportunity for the Railbelt—and the results show that tidal energy could, indeed, supply a significant portion of the Railbelt's electrical demand. However, much more analysis is needed before actual tidal energy integration could take place, such as detailed engineering studies that investigate sub-second dynamic response of the new technology, interconnection studies, financial feasibility studies, and more.

2 Methodology

In this section, we briefly characterize the tidal energy data used in the model, describe the development of the Railbelt power system operational model, and highlight the production cost modeling approaches used to evaluate tidal energy integration.

2.1 Basecase Formulation

The model used in our analysis expands on the production cost model developed by Denholm et al. (2022) to evaluate serving 80% of the Railbelt electrical load with renewable energy by 2040. We use the commercial production cost modeling tool PLEXOS by Energy Exemplar to run hourly unit commitment and economic dispatch simulations for a future year. The model ingests generator properties such as maximum nameplate capacities, heat rates, fuel costs, and seasonal water budgets for hydropower, as well as hourly time series like electrical load, wind, and solar PV production. It then runs an optimization procedure to determine the least-cost combination of all generator set points in each hour. This optimization produces an hourly time series for a wide variety of grid operation metrics like generation, fuel cost, and emissions by plant; curtailment of renewable resources; flow along transmission lines; and battery energy storage state of charge.

As in the previous renewable portfolio standard study (Denholm et al. 2022), we simplify the transmission topology of the Railbelt power system to a three-zone system. The zones are defined by the only two transmission bottlenecks in the system: the Alaska Intertie, which connects Fairbanks to the Anchorage region, and the Kenai Intertie, which connects the Anchorage region to the Kenai Peninsula. The GVEA zone is the Golden Valley Electric Association service territory on the north end of the Alaska Intertie. The Central zone includes the service areas of Chugach Electric Association, Matanuska Electric Association, the City of Seward municipal electric utility, and what was known as Municipal Light and Power until October 2020. This zone sits between the southern terminus of the Alaskan Intertie and the northern terminus of the Kenai Intertie and makes up 64% of the Railbelt's total electrical demand. The HEA zone is the service territory of the Homer Electric Association on the southern end of the Kenai Intertie. This zone also contains the interconnection points for the tidal energy studied in this report.

After extensive discussion with staff members at each Railbelt utility, we added the technical parameters of every thermal power plant in the model. The parameters include seasonal capacity, minimum stable level, heat rates, fuel costs, maintenance schedules, forced outage rates, emissions rates, and must-run statuses. Monthly energy budgets were incorporated for the hydropower plants at Bradley Lake, Cooper Lake, and Eklutna using publicly available data from the U.S. Energy Information Administration. Finally, we included existing or very likely to be built renewable energy plants and battery energy storage systems (BESS). These are listed in Table 1.

Table 1. List of Planned New Renewable Energy and Storage Projects

Plant name	Technology	Capacity	Location
Delta Wind Farm	Wind	90 MW (currently 1.9 MW)	GVEA
Eva Creek Wind Farm	Wind	25 MW	GVEA
HEA Wind Farm 1	Wind	31 MW	HEA
Nenana Solar	Solar utility PV	16 MW	GVEA
Homer Utility Solar	Solar utility PV	30 MW	HEA
Homer Residential Solar	Solar distributed PV	3 MW	HEA
Chugach BESS	Battery storage	70 MW, 4-hour	Central
GVEA BESS	Battery storage	100 MW, 2-hour	GVEA
HEA BESS	Battery storage	46 MW, 2-hour	HEA

Together with the thermal power plants throughout the Railbelt, these improvements constitute the Basecase scenario. Any gaps, such as monthly energy availability for the hydropower reservoirs, were filled with data from the U.S. Energy Information Administration. The 2035 Basecase electrical generation infrastructure for each zone, before adding any tidal capacity, is shown in Figure 2. All existing coal generation is assumed to be retired by 2035.

For more details on the Railbelt power system model, please reference Denholm et al. (2022).

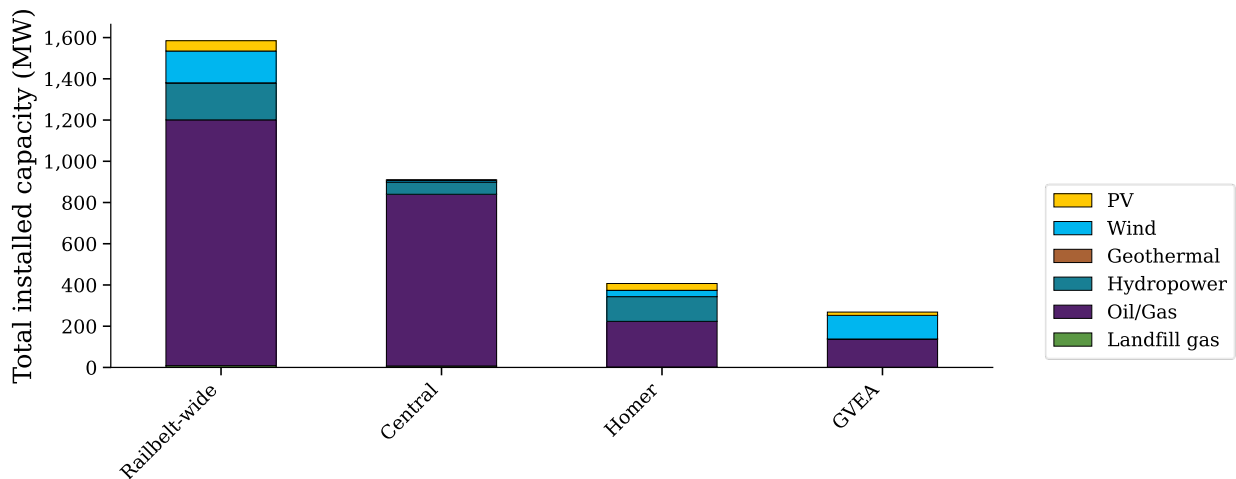


Figure 2. Total generation capacity, by region, for the Basecase system in 2035

2.2 Tidal Energy Data

Tidal energy resource data used in this study came from both the 2021 NREL measurements (Kilcher and McVey 2021) and from the NOAA C-MIST database (NOAA 2023)—a public repository of ocean current velocity data collected by NOAA. A comparison of the data from these two independent measurements, shown in Figure 3, highlights the predictability of tidal energy. The tidal harmonic fits are computed using the Python UTide package (Bowman 2022)

with no linear trend term. Both fits have high accuracy, explaining nearly 96% (independent, NOAA-fit) and 99% (concurrent, NREL-fit) of the variance in the 2021 measurements. In the case of the concurrent fit (black), the observed deviations from the “pure tidal signal” are most likely due to turbulence. Even more notable is the agreement between the NOAA-fit data (red) and the 2021 data (green). The fact that a harmonic fit to one month of data from 2005 predicts—with 96% accuracy—the timing and amplitude of the velocities 16 years later speaks to the remarkable predictability of tidal energy.

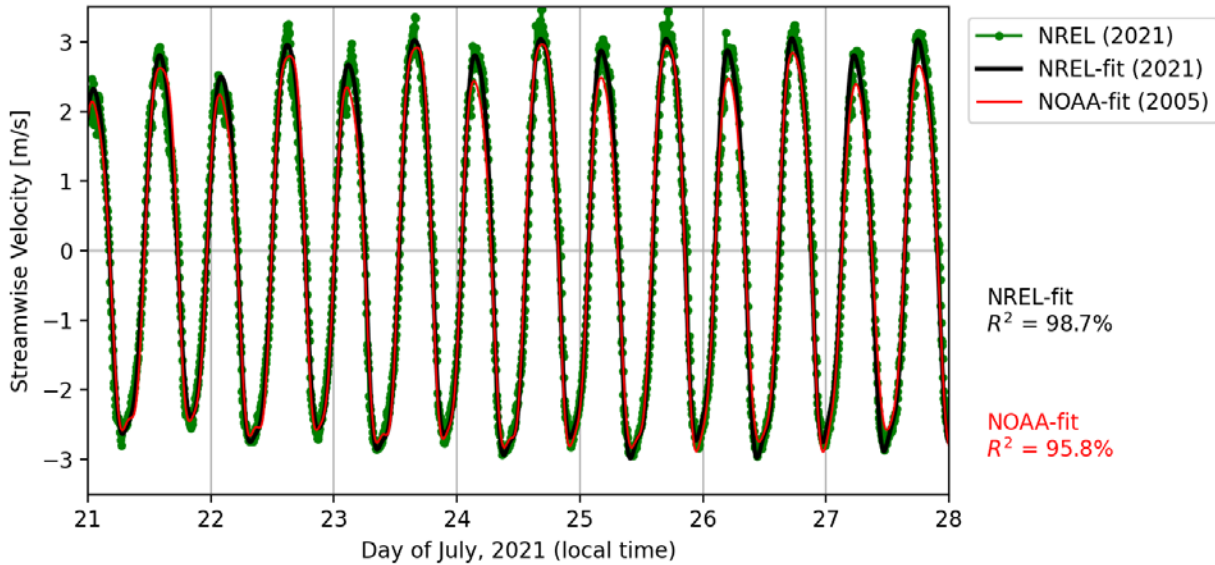


Figure 3. A comparison of measurements from NREL’s 2021 resource characterization project (green) with a tidal harmonic fit to that data (black) for East Foreland, and an extrapolation of a harmonic fit to data collected by NOAA at a nearby site in 2005

2.3 Tidal Power Model

We employed a three-region power curve to estimate power output for a single tidal energy device:

$$P(U(t)) = \begin{cases} 0 & U(t) < U_{cut-in} \\ \frac{1}{2}\rho AC_p U(t)^3 & U_{cut-in} < U(t) < U_{rated} \\ P_{rated} & U_{rated} < U(t) \end{cases} \quad (1)$$

where $U(t)$ is the inflow speed, $A = (d_{rotor})^2\pi/4$ is the device capture area (d_{rotor} is the rotor diameter), ρ is the density of seawater, and P_{rated} is the generator capacity. U_{rated} is the inflow speed where the power output reaches P_{rated} . For all scenarios we assumed that the device efficiency is $C_p = 0.42$, and we assumed that the cut-in speed, $U_{cut-in} = 0.1 \cdot U_{rated}$ (Lewis et al. 2021). Both assumptions are somewhat optimistic for the state of tidal energy technologies today, but this work is intended to be forward-looking.

We then assumed that the measured inflow $U(t)$ was representative of flow across an array of N devices so that we could estimate array power output according to:

$$\mathcal{P}_{\text{array}}(U(t), t) = N^*(t) \cdot (1 - \beta) \cdot P(U(t)) \quad (2)$$

where $N^*(t)$ is the availability of the N devices in the array (i.e., the number of operational devices vs. time), and we assumed array-wide losses—including wake losses, electrical losses, and other losses—of $\beta = 0.2$.

The assumption that $U(t)$ will apply to all devices in the array is a convenient simplification. Not only does the naturally occurring flow vary spatially in the channel, but—after turbines are installed—there will also be wake effects and flow diversion (i.e., flow around turbines and the entire array) that will create significant variability in the output of individual devices within the array. However, because a detailed array layout study and project cost estimates were beyond the scope of this study, we simply accounted for these wake losses as one of the major sources of energy loss included in β .

At present, there are no large- N tidal energy projects on which to base our assumption of $\beta = 0.2$. Instead, we note that wind energy resource assessments have calculated or used loss values from 8.8% to 23% (Musial et al. 2016; Stanley et al. 2022). We also note that, in the absence of cost or land-use constraints, array losses can be engineered by adjusting, for example, device spacing (wake losses) and transmission cable conductivity (electrical losses). In other words, we assume it is technically possible to design $\beta = 0.2$ tidal arrays up to 500 MW at each site in Cook Inlet, and we leave the assessment of the economic feasibility of these concepts for future work.

Tidal turbine rotors are sized to fit water depth constraints of the site, and the generators are sized to capture 95% of the energy ($P_{\text{rated@95\%}}$) that the rotor can generate at the site of interest (i.e., depending on the velocity distribution). The inflow speed at which the generator reaches this value of output is $U_{\text{rated@95\%}}$. We then assumed that arrays of these devices are deployed to create the array capacity of interest—i.e., power from a single device is scaled to match desired array capacity. We also assumed that $N^*(t)$ has a few devices going offline semi-randomly (preferentially in winter months) and that they are brought back online during summer months. When estimating array dimensions (shown in the last two columns of Table 2), we assumed simple rectangular grids with device spacing of $3 \cdot d_{\text{rotor}}$ and $10 \cdot d_{\text{rotor}}$ in the across-channel and along-channel directions, respectively. Additional details of device and array sizing can be found in Appendix A.

Table 2. Tidal Turbine Device and Array Sizing for Several Sites in Cook Inlet

Site	d_{rotor} [m]	$U_{\text{cut-in}}$ [m/s]	$U_{\text{rated@95\%}}$ [m/s]	$P_{\text{rated@95\%}}$ [MW]	N (100 MW) [$N_{\text{cols}} \times N_{\text{rows}}$]	CF_1	Array Dimensions (100 MW) W × L [km]
Fire Island	12	0.18	1.76	0.13	770 [70 × 11]	0.31	2.5 × 1.2
East Foreland	20	0.26	2.59	1.17	86 [22 × 4]	0.34	1.3 × 0.6
Anchor Point	20	0.16	1.58	0.26	384 [48 × 8]	0.19	2.8 × 1.4
Kennedy Entrance	100	0.11	1.13	2.41	41 [14 × 3]	0.18	4 × 2

3 Scenario Outline, Results, and Analysis

Taking a scenario-based approach, we demonstrate the impact of installing between 100 MW and 500 MW of tidal energy at the East Foreland in the HEA utility service territory. This is the most studied location by researchers and developers (Kilcher, Fogarty, and Lawson 2021). Once we built and validated a base case model of the Railbelt power system (as described in Section 2.1), we added theoretical tidal energy arrays and investigated the impacts. The method for producing the tidal energy generation profiles is outlined in Section 2.3.

To study the impact of injecting incrementally more tidal energy, simulations were run with tidal arrays of 100 MW, 150 MW, 175 MW, 200 MW, 250 MW, 300 MW, 400 MW, and 500 MW installed nameplate capacity. We chose a model analysis year of 2035 to allow sufficient lead time for these plants to be built, 13 years at the point of this analysis. Load profiles were calculated for each of the three Railbelt zones by scaling actual 2018 load profiles according to the Alaska Department of Labor’s countywide population growth projections (Howell and Sandberg 2022). Changing load shapes due to increased electrification of the energy sector (like household heating switching from gas to electric) as well as increased energy efficiency, are beyond the scope of this study. The projected peak loads in 2035 are 516 MW, 206 MW, and 83 MW in the Central, GVEA, and HEA zones, respectively. The projected peak loads occur between 6 and 8 p.m. in late January. Significant infrastructure improvements on the Kenai Peninsula would be necessary to incorporate the higher capacities of tidal energy while avoiding substantial curtailment of the energy production from the arrays. In this study we simulate two such improvements:

1. The upgrade of the Kenai Intertie from 115 to 230 kilovolts (kV), thereby increasing the line’s thermal rating (Tx) from 75 to roughly 150 MW.⁴ The map in Figure 1 shows the Kenai Intertie, which connects HEA to the rest of the Railbelt power system in the north.
2. The addition of a larger BESS at Soldotna on the Kenai Peninsula, for a total charge/discharge power of 150 MW. This power was chosen to match the assumed maximum transfer capacity of the Kenai Intertie, such that both pieces of infrastructure could offtake the same instantaneous tidal power at any given time.

In addition to the two improvements listed, we also studied a “copperplate” scenario that assigns unlimited transfer capacity to both Railbelt transmission lines (the Alaska and Kenai interties). These scenarios would require an extreme investment in the transmission corridor that is likely uneconomic; therefore, this scenario is simply meant to demonstrate the ideal utilization of the corridor while ignoring capital cost.

Table 3 summarizes the scenarios studied, and provides the prefixes used in all the plots in this report. The three-digit number after the underscore refers to the installed tidal energy capacity modeled in the scenario. For instance, “Tx-BESS_300” represents the power system

⁴ The Kenai Intertie is, and will continue to be, stability-limited rather than thermally limited. While initial estimates project that the new limit of the line will be 185 MW, this true value will not be known until a transfer capability study is completed around the time of construction. It will depend on the other generation and transmission resources available on the Railbelt system at that time. For the purposes of this exploratory study, we assume the more conservative value of 150 MW.

infrastructure as it existed in 2018, with load profiles scaled to 2035, Basecase infrastructure upgrades, the upgrade of both the BESS on the Kenai Peninsula and the Kenai Intertie, and the addition of 300 MW of tidal energy capacity at the East Foreland in the Cook Inlet. In addition, we included a single scenario with no tidal energy capacity to provide a Basecase.

Table 3. Scenario Description

Scenario Description	Scenario Abbreviation
Existing 2018 system electricity generation infrastructure with 2035 load and expected upgrades.	Basecase
Doubling the voltage of the Kenai Intertie from 115 to 230 kV. This assumes a doubling of the line's thermal rating from 75 to 150 MW.	Tx
Upgrading the BESS on the Kenai Peninsula to a total charge/discharge power of 150 MW and total capacity of 300 MWh. ⁵	BESS
Upgrading both the BESS and the Kenai Intertie.	Tx-BESS
Both the Kenai and Alaska interties are given unlimited transfer capacity.	Copperplate

⁵ The upgraded BESS would likely have to involve a new construction in addition to HEA's current BESS. The existing BESS is required to support system reliability standards and contractual energy transfer from Bradley Lake hydropower.

4 Results

4.1 Total Generation

Figure 4 illustrates the annual power generation broken down by technology type for select scenario combinations of tidal energy nameplate capacities and infrastructure upgrades within the Kenai Peninsula. Only the lowest and highest tidal capacities (100 MW and 500 MW) are shown for each scenario in the figure; see Appendix B for the full suite of results. The solid black line represents the Railbelt-wide native electrical load, while the dashed black line is native load plus the total energy used to charge the batteries. The total battery charging load (the difference between the solid and dashed black lines) is larger than the total battery discharge energy (the solid pink blocks in the generation stacks) because the round-trip efficiency is assumed to be 80%, not 100%. Tidal energy represents between 7% and 29% of the total power generation, depending on the installed tidal capacity and assumed upgrades. Landfill gas and geothermal provide consistent base load power, as their total output is identical across all scenarios. At the time of modeling (November 2022), all coal plants were assumed to be retired by 2035.

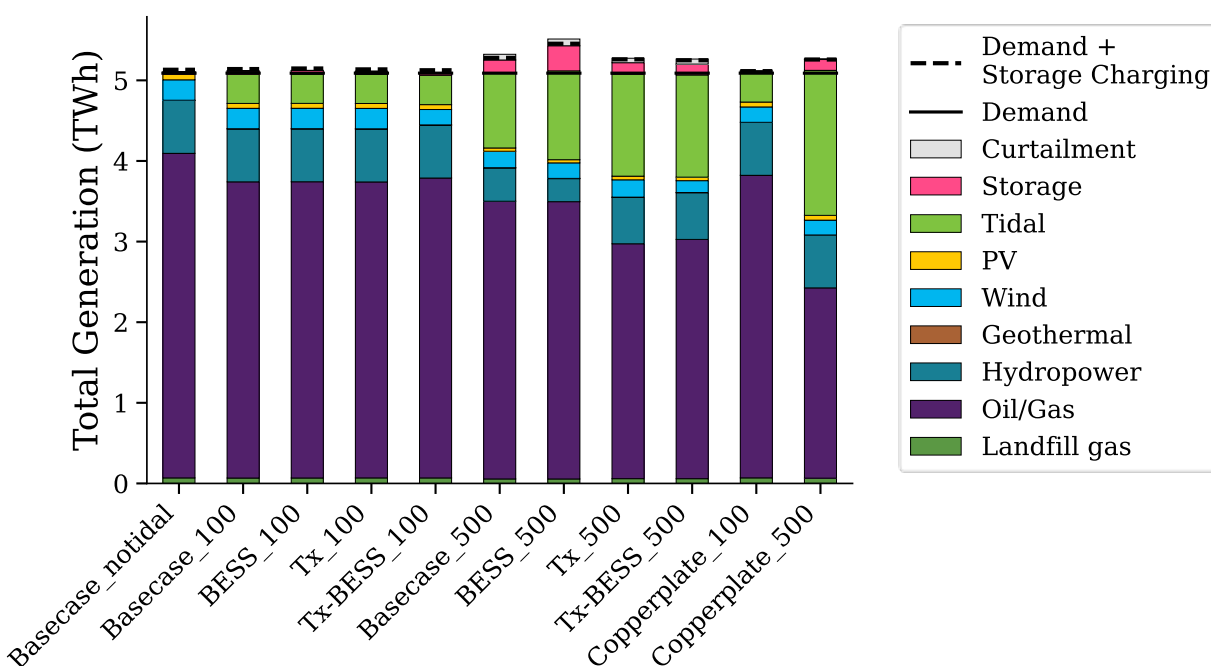


Figure 4. Total annual generation stacks for a representative subset of scenarios. The full set of total generation results can be found in Appendix B.

Figure 5 visualizes the results like Figure 4 but with a difference plot. Here, we subtract the total generation mix from the Basecase infrastructure from each scenario. Increased tidal energy injection largely displaces oil and gas generation across the Railbelt. However, at higher capacities, tidal energy also displaces hydropower. This is because the tidal energy is integrated into HEA's power grid on the Kenai Peninsula where thermal (oil and gas) generation is limited, and the Bradley Lake hydropower plant provides most of the electrical energy. Currently, local consumption of this plant's power is limited to HEA's capacity share of 14 MW. For tidal energy

to displace hydropower, the present-day financial contracts that govern the operation of Bradley Lake would have to change significantly. Because this study is concerned with techno-economic feasibility and not with capturing all current contractual capacity share obligations, we assume these changes happen by 2035.

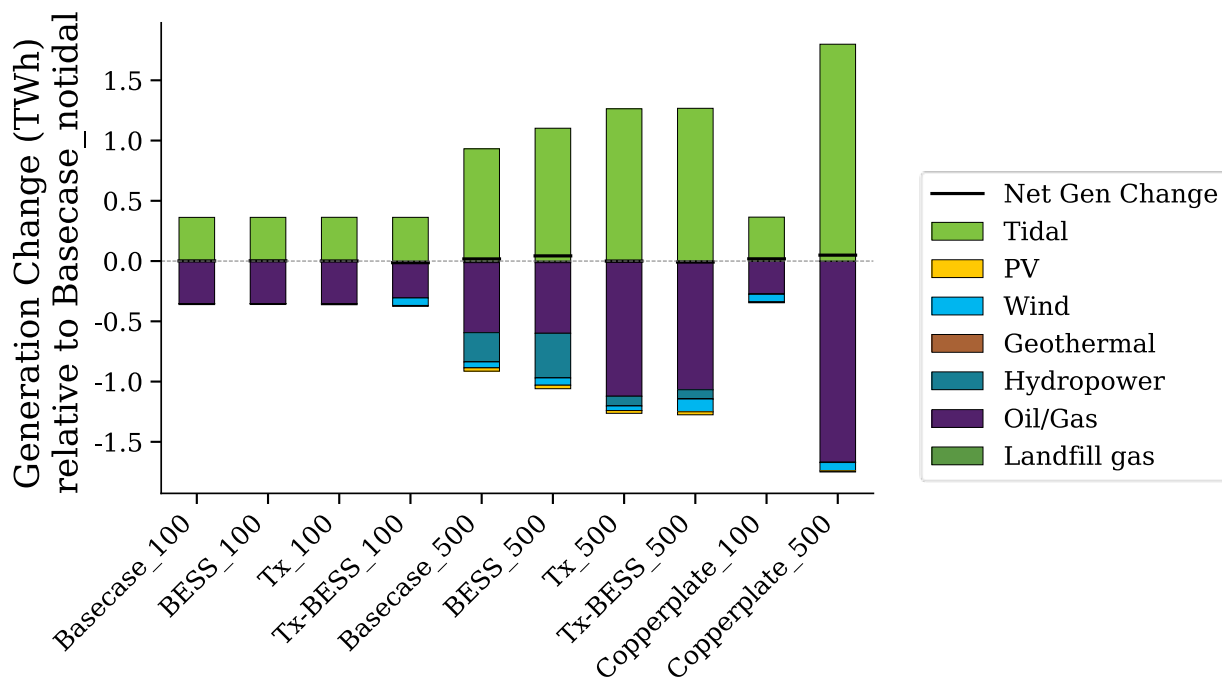


Figure 5. Total annual generation stacks for a representative subset of scenarios, compared to the Basecase infrastructure with no tidal energy capacity. The full set can be found in the Appendix.

Without expansion of the Kenai Intertie, large amounts of instantaneous tidal power cannot serve loads in the Central and GVEA regions, which contain more thermal generators. The system must instead curtail some of the zero-marginal-cost energy⁶ produced by the tidal and hydropower facilities. Because the Bradley Lake plant can store its energy for a time when tidal energy is minimal, the model values the variable, inflexible tidal energy more highly and strives to curtail it last. Therefore, to minimize curtailment of tidal energy, the system reduces hydropower generation. This can be seen in the “Basecase_100” and “Basecase_500” stacked bars in Figure 5, which compares total annual generation of each scenario relative to the Basecase with no tidal energy installed. In the Basecase_100 scenario, 97% of the additional tidal energy displaces oil and gas generation, 1% displaces hydropower, and 2% leads to increased battery charging. However, the system only has so much thermal generation that can be displaced, so in the Basecase_500 scenario, these numbers shift to 77% oil and gas displacement, 20% hydropower displacement, and 3% increased battery charging.

⁶ Zero-marginal-cost energy implies that unused energy does not increase systemwide production cost. However, individual utilities may still have to pay for unused (curtailed) energy based on their existing “take-or-pay” contracts.

Figure 5 also shows some wind curtailment and a small amount of solar PV curtailment, primarily in the high tidal capacity scenarios. We assume zero variable costs for these technologies, so the model generally treats curtailment of wind, solar PV, and tidal energy as equivalent.⁷ This means that, absent other constraints, the optimization model sees no difference between curtailing any of these resources. However, the upgrade of the BESS in HEA does increase wind curtailment, which can be seen by comparing the “Tx_100” and “Tx-BESS_100” bars in Figure 5. This is likely because the extra flexibility provided by the larger battery allows for more periods of direct competition between tidal energy in HEA and wind energy elsewhere on the Railbelt.

By contrast, when the Kenai Intertie is upgraded, the injected tidal energy has more opportunity to displace thermal generation outside of HEA. This is because the additional transfer capacity allows more export of tidal energy from the Kenai Peninsula to the Central region, which contains the majority of the Railbelt’s thermal generation. Consequently, the stacks in Figure 5 for all scenarios with “Tx” or “Tx-BESS” upgrades show little to no change in hydropower generation.

The value of upgrading the transfer capacity of the Kenai Intertie is a major theme in these findings. Beyond allowing significantly more tidal energy to displace thermal generators outside of HEA, it greatly impacts curtailment of the tidal resource.

4.2 Curtailment

Figure 6 shows how higher tidal energy deployment leads to increasing levels of curtailment. (Because the purple “Tx” values are almost identical to the red “Tx-BESS” values, the line is difficult to see.) As stated previously, curtailment refers to extra available renewable energy that could not be injected into the grid due to transmission constraints or insufficient demand. The black dashed line denotes 5% curtailment; curtailment above this number may lead a given technology to lose economic viability. However, many countries have recorded a wide range of renewable energy curtailment between 0% and 30% (Bird et al. 2016), and an “acceptable level” of curtailment depends on the marginal cost of generation in each system. Therefore, the 5% value chosen here is meant to be used as a benchmark to aid comparison of the study scenarios and does not reflect a techno-economic finding from this study.

⁷ The various power purchase agreements associated with zero-marginal-cost resources like hydro, tidal, wind and solar PV may affect the order in which resources are curtailed. Because this study does not attempt to capture existing contracts that may change by 2035, we only assign costs associated with physical production of electricity.

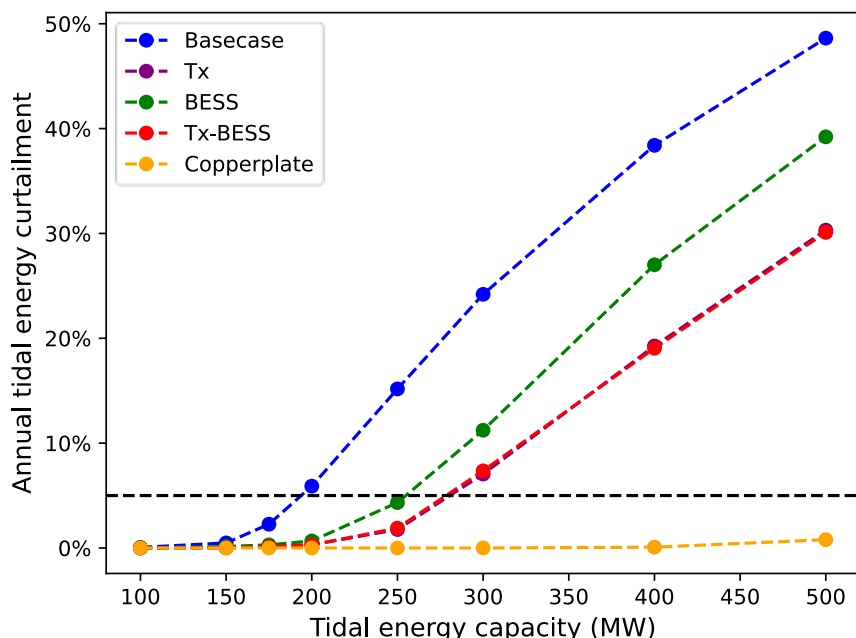


Figure 6. Total annual tidal energy curtailment as a function of both installed capacity and infrastructure upgrade scenario. The black dashed line represents 5% curtailment. Note the “Tx” values are almost identical to the “Tx-BESS” values.

Without any infrastructure upgrades (the Basecase, or the blue line in Figure 6), the system barely surpasses 5% tidal energy curtailment at 200-MW deployment. Keep in mind that the average capacity factor of the East Foreland tidal energy project is 41%. That means that a 200-MW deployment injects only ~81 MW on average, which matches HEA’s current peak demand.

The upgrades of BESS in both the HEA and the Kenai Intertie increase the amount of tidal energy that can be deployed while keeping tidal energy curtailment below 5%. When the power of the BESS in HEA is increased, the system can accommodate between 250 and 300 MW of tidal energy without experiencing more than 5% curtailment. Doubling the transfer capacity of the Kenai Intertie has a slightly greater impact on curtailment reduction, but the system still surpasses 5% tidal energy curtailment at 300-MW tidal energy capacity. Adding both the upgraded BESS and doubling the Kenai Intertie was found to have very similar results to just doubling the Kenai Intertie scenario. Again, while integrating these levels of capacities would likely require changes to how Bradley Lake and the Kenai Intertie are operated, such contractual changes would be advisable if they reduced systemwide production costs.

The copperplate scenarios (unlimited transfer capacity for both the Alaska and Kenai interties) show little to no curtailment across all tidal energy capacities. This suggests that transmission limits are almost solely responsible for tidal energy curtailment. In addition to transmission expansion, more flexible thermal units could also reduce curtailment. However, we keep the technical characteristics of thermal units constant across all scenarios. These characteristics include quadratic heat rate curves that capture the lower efficiencies thermal units experience during partial loading. Higher variable renewable deployment leads to lower capacity factors for thermal units, meaning they operate in lower-efficiency states more often than in the Basecase scenario.

4.3 Impact of Tidal Energy on Systemwide Generation Cost

As shown in Figure 7 and Figure 8, fuel cost savings are directly proportional to tidal energy injected into the Railbelt grid. The black dashed line in both figures represents the annual fuel cost of the system in 2035 with no tidal energy deployment. However, fuel cost savings are determined by more than the quantity of tidal energy that serves load somewhere in the Railbelt. For a given level of tidal energy injection, the fuel cost savings vary widely depending on the infrastructure scenario. For instance, even though the system successfully injects 633 GWh of tidal energy in the scenario with 175 MW of tidal energy and the HEA BESS upgrade, fuel costs still total \$524 million. By contrast, in the scenario with the Kenai Intertie upgrade, the system results in a 5% lower total fuel cost (\$496 million) with a similar amount of tidal energy injection (634 GWh). These points are emphasized with the oval in Figure 8. The additional transfer capacity of the Kenai Intertie allows the tidal energy to displace more thermal generation in the Central region, thus lowering fuel costs.

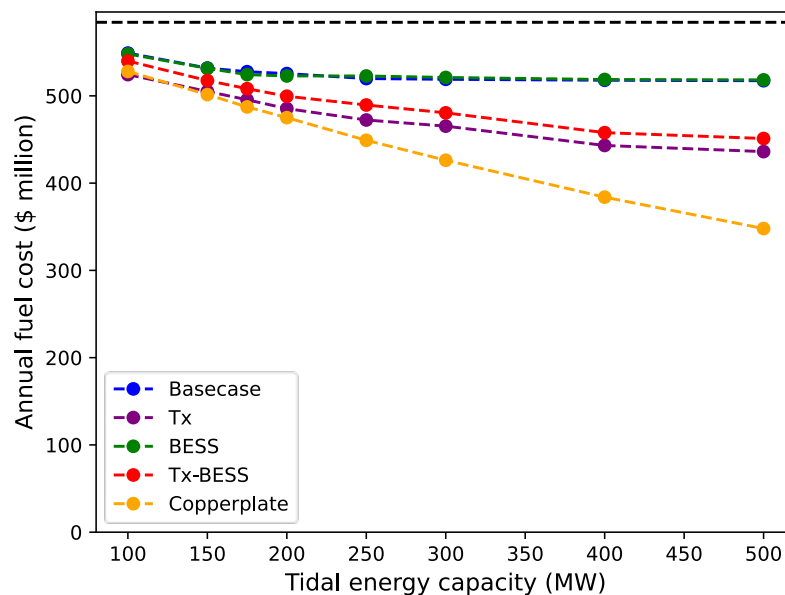


Figure 7. Total systemwide fuel cost, as a function of installed tidal capacity and infrastructure upgrade scenario. The black dashed line shows the cost with no tidal energy deployment.

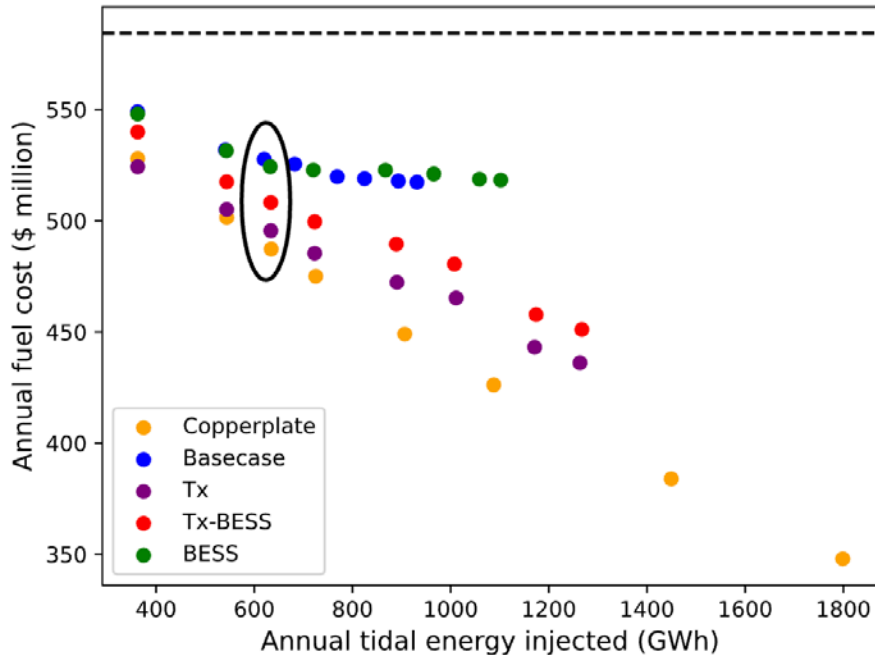


Figure 8. Total systemwide fuel cost as a function of total tidal energy injected (i.e., tidal energy that was not curtailed). The oval highlights the impact of various infrastructure upgrades on fuel cost reduction, while keeping the total tidal energy injected constant. Upgrading the Kenai Intertie has the largest impact on fuel cost reduction.

Investigating the difference in fuel costs between scenarios further highlights the importance of the Kenai Intertie upgrade in reducing fuel costs. Figure 9 shows the annual fuel cost savings for each infrastructure upgrade scenario relative to the tidal Basecase with no upgrades. While a larger battery in HEA slightly reduces fuel costs, this effect is capped at around \$3.3 million, and it actually reverses at 250-MW tidal capacity deployment. A monotonic increase in fuel cost savings with increasing tidal capacity would be expected and is what we observe for the other infrastructure scenarios. The decrease in fuel cost savings for the BESS case may indicate a quirk of the simulation in which certain thermal units are committed during more hours in the higher tidal capacity scenarios. More analysis would need to be done to determine the exact reason for the decrease. However, this pattern is quite small relative to the other scenarios.

Note that in this section—and in the entire study—we model only variable operational costs. Capital and fixed operations and maintenance costs associated with the deployment of new generation resources or transmission upgrades are outside the scope of a production cost modeling study. For an assessment of these costs in the context of an 80% by 2040 renewable portfolio standard for the Alaskan Railbelt, see Denholm, Schwarz, and Streitmatter (2024).

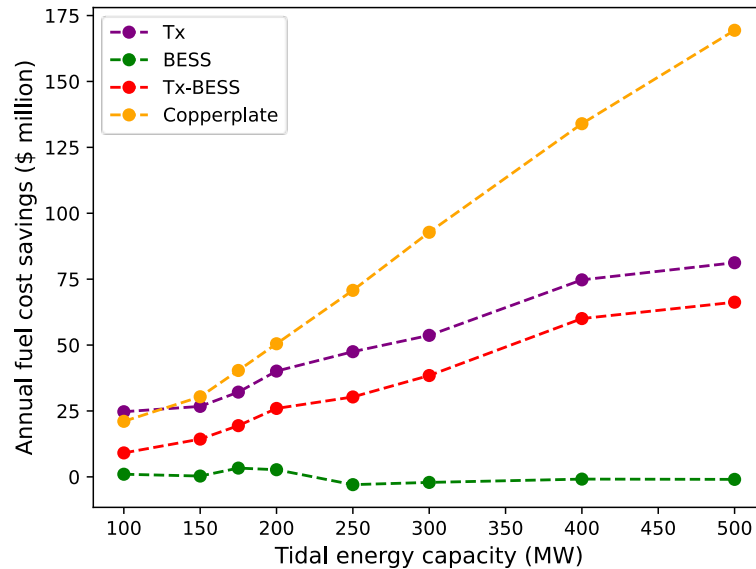


Figure 9. Similar to Figure 7, but showing the fuel cost savings from the no-infrastructure-upgrades Basecase. The x-axis shows tidal energy deployment, rather than tidal energy injection.

By contrast, upgrading the Kenai Intertie saves over \$40 million annually at 200-MW tidal energy deployment, and \$81 million annually at 500-MW deployment. HEA has a limited thermal power plant fleet and therefore limited opportunities for tidal energy to displace fossil fuel on the Kenai Peninsula. The more tidal energy that can reach the central and northern Railbelt utility regions, the more total fuel it can displace. In summary, the transmission upgrade has two important effects: (1) it reduces tidal energy curtailment and (2) for a given level of curtailment, it displaces more thermal generation by transporting tidal energy to Anchorage and the Mat-Su valley.

The other significant component to systemwide production cost, besides fuel, is the startup and shutdown costs of thermal generators. These are the major costs associated with cycling thermal plants. Increasing the variable generation on a system sometimes increases startup and shutdown costs, as natural gas plants may have to cycle more to accommodate larger fluctuations in net load (Lew et al. 2013). Net load refers to raw electrical demand with variable generation like wind, solar, and tidal subtracted. As shown in Figure 10, Basecase tidal energy injections below 700 GWh lead to higher cycling costs compared to the Basecase with no tidal energy capacity, but this effect reverses above 700 GWh. Once again, the black dashed line shows the startup and shutdown cost for the Basecase scenario with no tidal energy. The cycling costs are lower in all copperplate scenarios, as the elimination of all transmission bottlenecks reduces the need for flexible operation of thermal plants. However, higher tidal capacities require more flexible thermal plants. This is because we simulate larger arrays by scaling the same diurnal tidal profiles, so the ramps in available tidal energy become steeper, and a larger capacity of quick-response, dispatchable thermal and battery capacity becomes necessary to fill in the gaps. Interestingly, at the highest tidal energy injection, the cycling costs in the copperplate scenario match the Basecase with no tidal energy almost exactly. There is no clear pattern between total tidal energy injected and cycling costs for the other scenarios. These effects are relatively small,

however, as the startup and shutdown costs are roughly a full order of magnitude lower than the fuel costs.

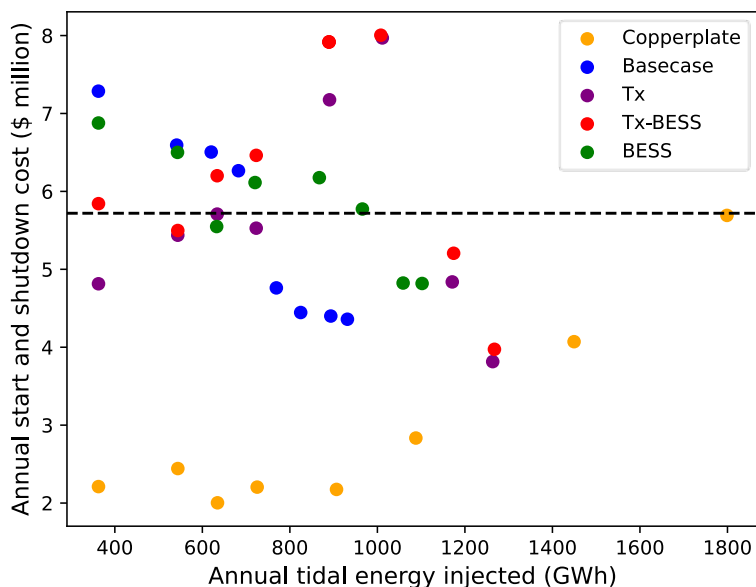


Figure 10. Total systemwide startup and shutdown costs (also referred to as cycling costs) as a function of tidal energy injected and infrastructure upgrade scenario for 2035 infrastructure with no new wind or solar PV. The black dashed line shows the value for the scenario with no tidal energy. Consistent with other metrics, the copperplate scenarios have the highest impact on this cost category. However, the impact is an order of magnitude smaller than that for fuel cost.

4.4 Impact of Tidal Energy on Thermal Power Plant Emissions

Figure 11 plots the annual power plant emissions (carbon dioxide [CO₂], ammonia [CH₄], and nitrous oxide [N₂O]) across all studied scenarios. As emissions produced are a direct consequence of fuel burned, the trends follow similar patterns to the fuel costs shown in Figure 9. As expected, as more tidal energy enters the Railbelt grid—via larger installed tidal plants, infrastructure upgrades, or both—the system emits less pollution. However, due to differential fuel prices and differences in emissions rates for each technology, the trends in emissions reduction differ for each pollutant. The emissions rates used in this study, measured in tons of pollutant emitted for each unit of electricity produced, are shown in Table 4.

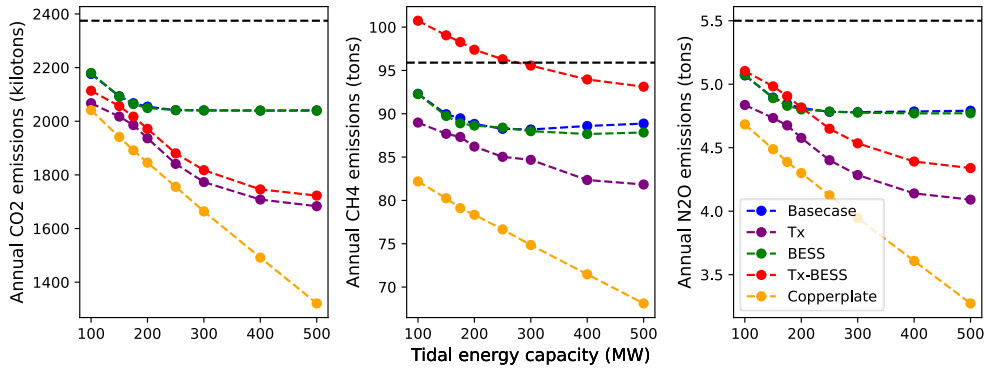


Figure 11. Total power plant emissions under each tidal energy and infrastructure upgrade scenario. As before, the black dashed line represents the value in a system with no tidal energy. From left to right, the panels show CO₂, CH₄, and N₂O emissions. The y-axis lower limit of zero is removed to increase clarity.

Table 4. Emissions Rates for Different Thermal Power Plant Technologies in Alaska

All values are in kg/MWh. Emissions rates for thermal generators in Alaska were drawn from the U.S. Environmental Protection Agency’s (EPA’s) eGRID 2005 (EPA 2023).

Pollutant	Gas	Oil
CO ₂	576	747
CH ₄	0.01143	0.3234
N ₂ O	0.00113	0.01379

The Kenai Intertie upgrade has a larger impact on emissions than the BESS upgrades, and the copperplate scenario leads to the lowest emissions of all. Upgrades to the Kenai Intertie will allow southern Cook Inlet tidal energy to displace more thermal generation in the central and northern regions of the Railbelt. Conversely, the BESS upgrade has a limited impact on further emissions reduction (as shown by the near-identical values of the green and blue lines in all three panels of Figure 11).

4.5 Impact of Tidal Energy on Transmission Utilization

Figure 12 shows a flow duration curve for the Kenai Intertie for all tidal deployment scenarios with tidal capacity fixed at 150 MW. To create such a curve, the annual chronological 8,760-hour time series is sorted from highest to lowest individually for each scenario. The x-axis represents the portion of the year that the Kenai Intertie flow is greater than or equal to the value on the y-axis. As a reminder, the “Basecase” and “BESS” scenarios model the existing line limit of 75 MW, the “Tx” and “Tx-BESS” scenarios model the line with a limit of 150 MW, and the line has unlimited transfer capacity in the “Copperplate” scenario. Once again, values for the “Tx” and “Tx-BESS” scenarios are nearly identical, so the purple line is hidden. Similarly, the green line is mostly hidden behind the blue line, since the Kenai Intertie flows are almost the same in the “BESS” and “Basecase” scenarios. The differences arise when we incorporate

expansion of the line. This means that additional BESS capacity does not alleviate congestion along the line.

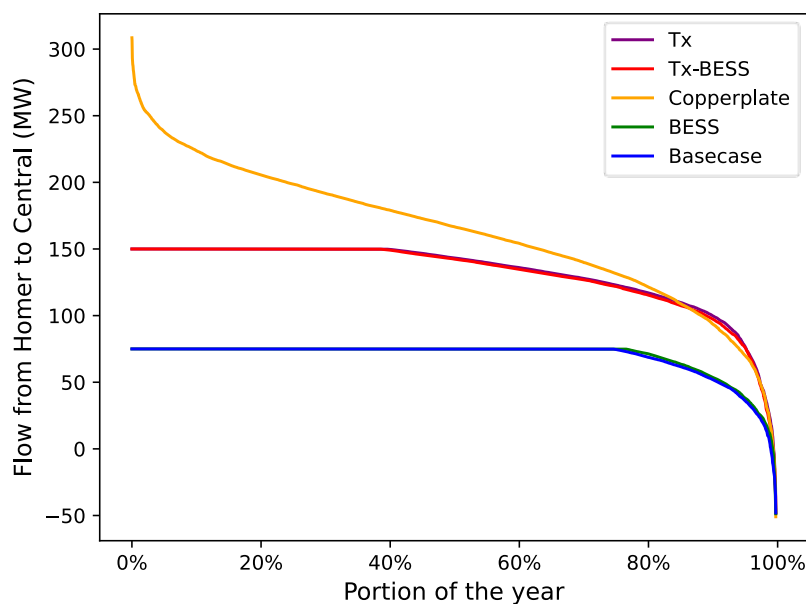


Figure 12. Flow duration curves for the Kenai Intertie in the 150-MW tidal deployment scenarios. Note the “Tx” values (purple) are almost identical to the “Tx-BESS” values (red). Additionally, the “BESS” values (green) are almost identical to the “Basecase” values (blue).

The Kenai Intertie is congested during 75% of the year (6,573 hours) when the line is not upgraded, and 39% of the year (3,435 hours) when the line is upgraded. Recall from Figure 6 that the system curtails little to no tidal energy in the 150-MW cases across all scenarios. This means that all the tidal energy is either consumed locally on the Kenai Peninsula, stored in the HEA battery, or exported along the Kenai Intertie up to the Central region. Even at this relatively low tidal capacity, however, the larger capacity line leads to significantly fewer hours of line congestion. For less than 1% of the year (30–67 hours), the intertie shows a negative flow. This represents HEA importing power from the Central region and most likely occurs during slack-tide events. These negative flows would likely only occur if the contracted use of Bradley Lake hydropower was changed, so more of its energy was used locally rather than exported north along the Kenai Intertie.

Figure 13 shows the Kenai Intertie flow duration curves for all tidal capacity scenarios. The number of congested hours increases with increasing tidal capacity, as the amount of available tidal energy surpasses the line’s transfer limits and the load on the Kenai Peninsula. At 200-MW tidal capacity, the intertie is congested during 89% of hours in the “Basecase” scenario; this value reaches 99% at 250 MW and higher capacities. When the intertie is upgraded, it is only congested for about half the year at 250-MW tidal capacity and reaches a maximum of 78% congestion hours at 500-MW tidal capacity.

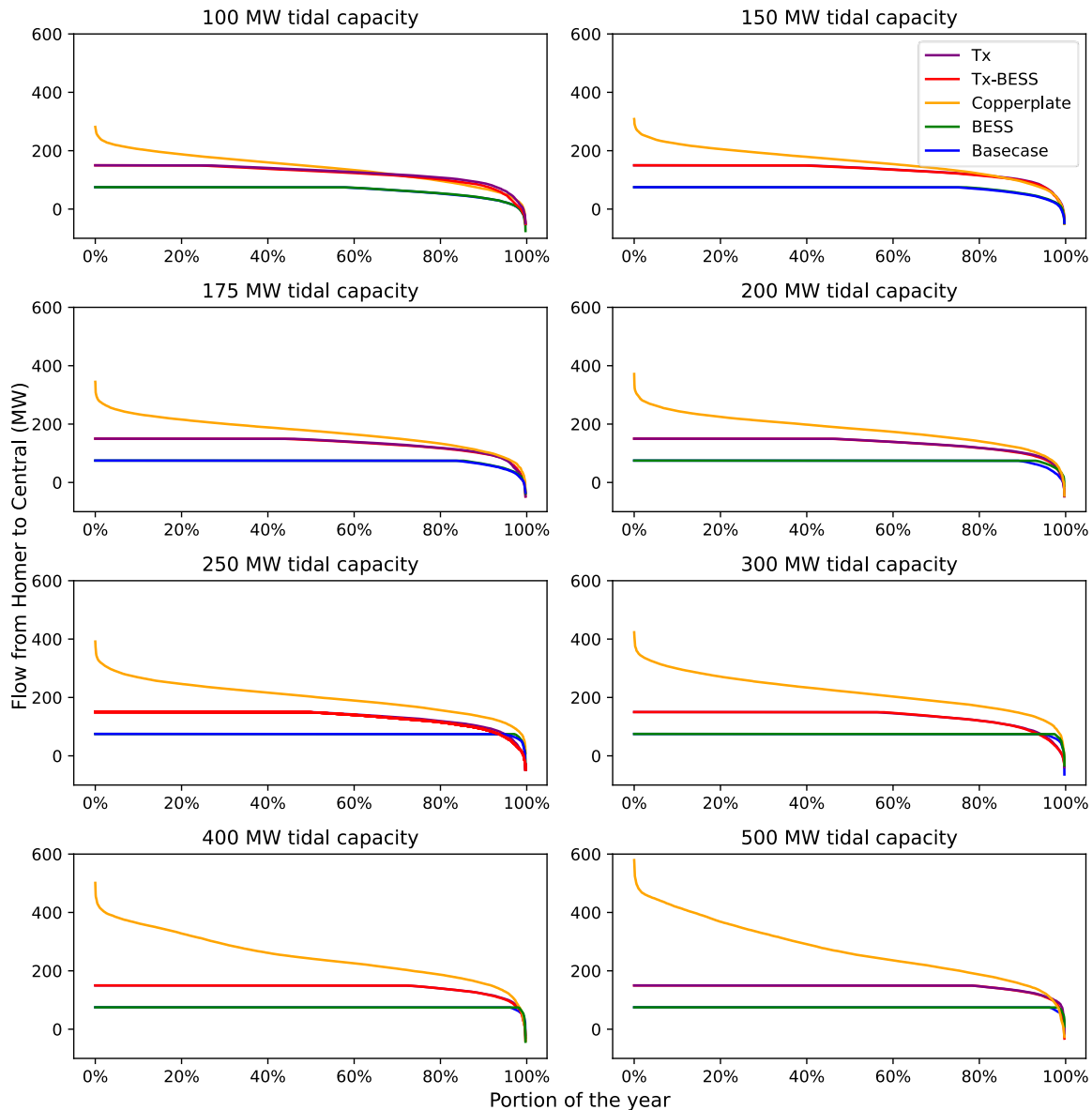


Figure 13. Similar to Figure 12, but showing flow duration curves for all tidal capacity scenarios

Interestingly, the 200-MW scenarios are where we see the largest difference between the “Basecase” and “BESS” scenarios (blue and green lines, respectively). The system uses the intertie’s export capability more heavily during more hours in the BESS scenario. This is because the battery can store tidal energy and discharge it during periods that exhibit non-congestion along the intertie and slack tide. The difference diminishes at higher tidal capacities because there is enough tidal energy available to fill the entire export capability of the line during most hours, regardless of the BESS capacity.

Finally, the utilization of the intertie in the copperplate scenarios illustrates what transfer capacity would lead to the cheapest operations at each level of tidal capacity. The maximum export value is roughly 423 MW at 300-MW tidal capacity and below, and it reaches 579 MW in

the 500-MW tidal capacity scenario. Of course, developing the transmission corridor to this extent would not likely be economic, so some tidal energy curtailment would be expected at these high capacities. This highlights the earlier finding that the difficulty in exporting tidal energy out of the Kenai Peninsula is the greatest barrier to large-scale tidal deployment in the Cook Inlet.

5 Investigation of Tidal Array Placement Along the Cook Inlet

While tidal energy is fully predictable, the fact that it drops to zero twice a day means it is a highly variable resource that still must be managed by other, dispatchable resources. One key method to reduce the variability of energy sources like tidal is to take advantage of geographically diverse resources (Klima and Apt 2015). Spreading out variable generation plants across a utility's footprint often leads to a smoother aggregate output that is easier to manage with dispatchable thermal resources. The process of using spatial heterogeneity to combine individual variable resources into a less variable aggregate output is often referred to as geographic smoothing.

The differential timing of tidal cycles in the Cook Inlet provides opportunities for geographic smoothing, even within its relatively small footprint. Figure 14 shows three theoretical locations for tidal energy plants (East Foreland, Anchor Point, and Kennedy Entrance), scattered across the Cook Inlet, that would both maximize geographic heterogeneity and allow for relatively short interconnections⁸ to the existing power system. A fourth site (Fire Island) is also shown and discussed in a later analysis. Even in the relatively small area of Cook Inlet, the phase difference between tidal cycles allows for geographic smoothing. This phase difference is illustrated with tidal current speed profiles for each site in Figure 15. These phase differences are consistent over the course of a given year and over decadal timescales.

⁸ The Kennedy Entrance site would require 40+ miles of subsea cables to reach the HEA transmission system. Therefore, tidal energy deployment at this site would likely cost significantly more than at the other locations mentioned.

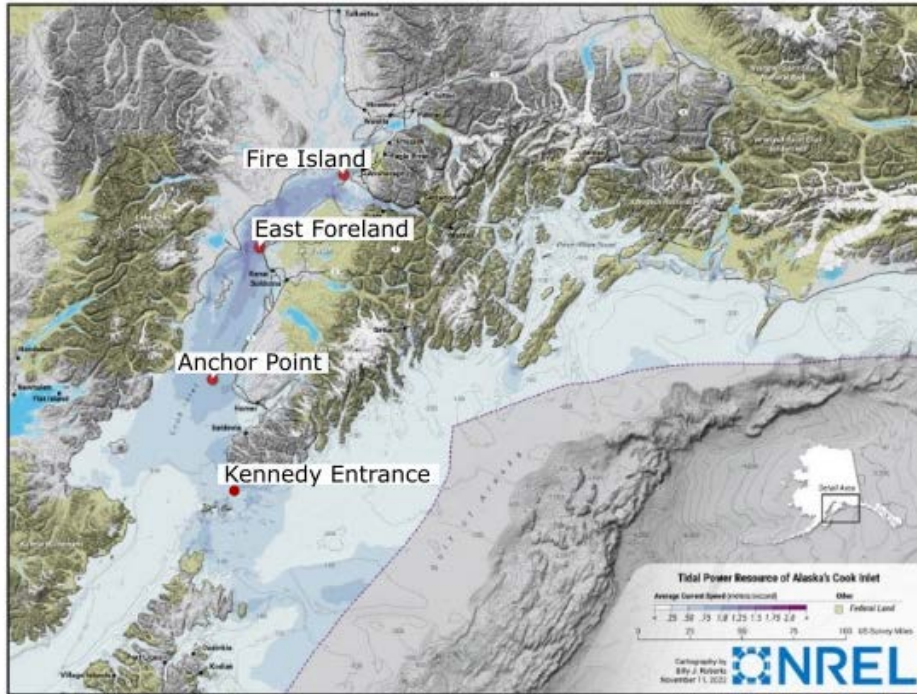


Figure 14. Map showing four theoretical locations for tidal energy throughout the Cook Inlet.

Map by Billy J. Roberts, NREL

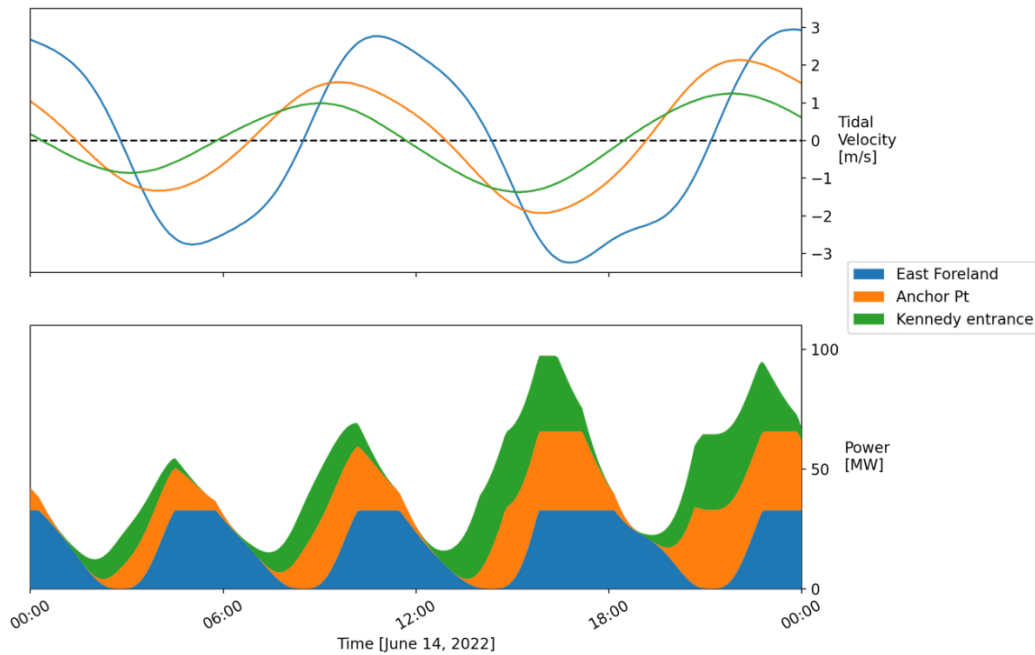


Figure 15. Tidal current speed profiles (upper panel) for the three southern Cook Inlet sites. The phase difference in tidal cycles means that the combined power output from the three sites (lower panel) is never zero. In this case, each site has 33 MW of capacity, for a total of 99 MW.

The previous analysis assumed all tidal energy would be placed off the East Foreland near Port Nikiski, as this location has been most significantly studied by researchers and developers (Kilcher, Fogarty, and Lawson 2021). In this section, we investigate how spreading capacity across these sites allows the Railbelt power system to integrate more tidal energy with less curtailment.

Figure 16 shows the total annual tidal energy curtailment when capacity is distributed evenly between the three sites. Unsurprisingly, when the three profiles are combined, the Railbelt power system can absorb significantly more tidal energy. At an installed capacity of 250 MW, the three-way split scenario experiences 3.5% tidal energy curtailment, whereas curtailment reaches above 15% in the scenarios with all 250 MW placed at a single site; that is, the Railbelt power system can integrate more than 250 MW of tidal energy while keeping tidal curtailment below 5% when all three sites are combined. However, this value drops to less than 200 MW of installed tidal capacity when only Anchor Point or East Foreland are used, and around 175 MW when only the Kennedy Entrance location is used. The Kennedy Entrance location appears to line up least often with peak net load, as the system reaches higher levels of tidal curtailment when the capacity is installed there—although, this is due to the historical tidal data year chosen. In this year, the tidal cycles at the East Foreland happened to serve net load peaks slightly better than those at Kennedy Entrance. Figure 17 characterizes the correlation between the four tidal energy sites studied and total net load across the Railbelt. As shown, the correlation values between all tidal sites and net load are near zero. However, the correlations and anti-correlations between tidal energy profiles are significant.

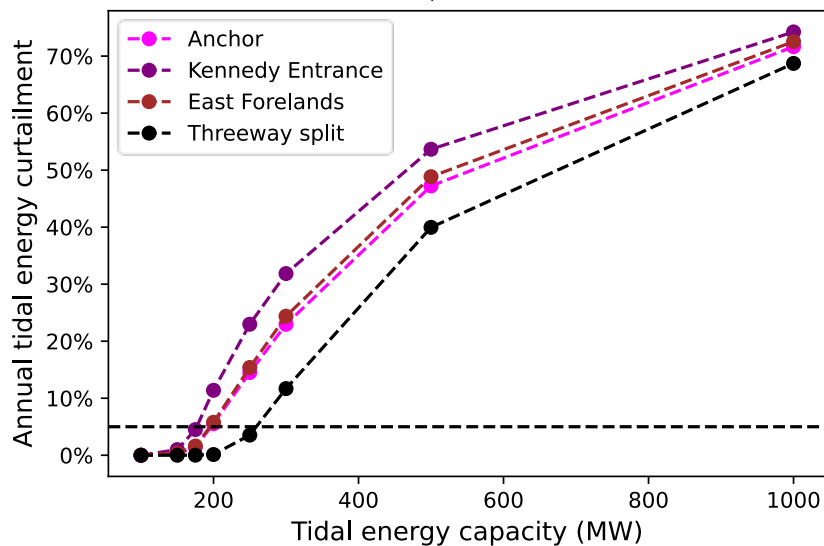


Figure 16. Total annual tidal energy curtailment with capacity all placed at each of the three southern Cook Inlet sites, and an even split between the three sites. The flat black dashed line represents 5% curtailment. Above this number, the curtailment technology may lose economic viability.

	East Forelands Tidal	Fire Island Tidal	Anchor Point Tidal	Kennedy Entrance Tidal	Railbelt net load
East Forelands Tidal	1.00	0.19	0.30	-0.31	0.00
Fire Island Tidal	0.19	1.00	-0.42	0.70	0.01
Anchor Point Tidal	0.30	-0.42	1.00	-0.44	-0.00
Kennedy Entrance Tidal	-0.31	0.70	-0.44	1.00	-0.01
Railbelt net load	0.00	0.01	-0.00	-0.01	1.00

Figure 17. Correlogram between tidal energy profiles for all four sites studied and total Railbelt-wide net load. The Kennedy Entrance site is the most negatively correlated with the other sites. It is also the site most negatively correlated with net load, though this value is near-negligible.

With further investigation and analysis, it was found that distributing capacity to a location near Fire Island near the Port of Anchorage at the head of the Cook Inlet has a more significant impact on curtailment reduction. A tidal energy plant located near Fire Island would inject its power directly into the central region of the Railbelt, thereby bypassing the Kenai Intertie. Avoiding this transmission limitation by placing all capacity at Fire Island would allow significantly more tidal capacity to be integrated while maintaining curtailment below 5% with up to 500 MW, as opposed to 175 MW if all were placed at the East Foreland location, as assumed in the previous section. Splitting the capacity evenly four ways between Fire Island and three sites in the southern Cook Inlet results in moderate curtailment values between the extremes of 500 MW or 175 MW. This solution is limited, however, as this amount of installed capacity near the Port of Anchorage may not be feasible because of the depth in the upper inlet and the conflict with vessel traffic. It remains an interesting solution to congestion on the intertie and is worthy of further investigation in the effort to optimally position tidal arrays for maximum cost benefit.

6 Summary and Conclusion

This is the first study to investigate the value of substantial, megawatt-scale tidal energy development in Alaska’s Cook Inlet. We found that there are significant opportunities to capture the resource available in the region. While the reported theoretical resource is >18,000 MW, this study found that the existing electrical transmission constraints—specifically, those associated with the Kenai Intertie—impose a practical limit of approximately 200 MW. These levels of tidal energy capacity have the potential to reduce fuel costs in Alaska while also reducing carbon emissions and increasing the energy independence of the state.

This study also highlights the need for transmission line upgrades. These upgrades would allow for the energy produced by the tidal arrays to be used at locations further north along Alaska’s Railbelt electrical grid. By doubling the current transmission line rating, the tidal energy capacity could be increased nearly 50% to 300 MW with similar curtailment values, contributing just under 20% of the total Railbelt load and reducing annual CO₂ emissions by more than 20%. Further investment into transmission line upgrades, as demonstrated by the copperplate scenarios, show a corresponding value in decreasing both energy costs and CO₂ emissions. Additional dispatchable load near the site of the tidal generation would also allow the Railbelt system to integrate larger capacities of tidal energy.

This work also shows that it is possible to increase the total installed capacity—without major transmission upgrades—by distributing tidal arrays along the inlet. This approach takes advantage of the fact that the tidal currents peak at different times along the inlet. While a study of the costs of these different approaches is beyond the scope of this work, these initial results suggest an optimized geographic layout could have significant value in terms of installed capacity limits and techno-economic viability.

Unfortunately, this study was not able to fully evaluate and properly demonstrate one of tidal energy’s major benefits that sets it apart from other variable energy technologies: its predictability. Doing so would require modeling wind and solar PV forecast error in a two-stage, day-ahead/real-time modeling framework, which would in turn require accurate forecast data for wind and solar PV in Alaska. In this framework, tidal energy would be assigned its appropriate advantage from perfect forecasting; currently, all variable generation is assumed to have perfect forecasts. Unfortunately, such forecast data are not yet available in the region.

Taken together, this work provides a basis for understanding the grid constraints for developing tidal energy in the Cook Inlet. The 200-MW “practical limit” suggests that >100 MW of tidal energy capacity can be installed in Cook Inlet without major disruptions to system operations. However, this amount of power is greater than HEA’s average (50 MW in 2020) and projected peak load (83 MW), so projects at this scale would need to involve contracts with other utilities or industrial power consumers (Denholm et al. 2022). Finally, the question of capital investment costs is beyond the scope of this study. For a proper evaluation of the long-term planning costs associated with decarbonizing Alaska’s Railbelt power grid, see Denholm, Schwarz, and Streitmatter (2024) and Cicilio et al. (2024).

References

- Alyeska Pipeline. 2023. “Monthly Throughput.” Accessed May 19, 2023. <https://www.alyeska-pipe.com/historic-throughput/>.
- Bird, Lori, Debra Lew, Michael Milligan, E. Maria Carlini, Ana Estanqueiro, Damian Flynn, Emilio Gomez-Lazaro, et al. 2016. “Wind and Solar Energy Curtailment: A Review of International Experience.” *Renewable and Sustainable Energy Reviews* 65: 577–586. <https://doi.org/10.1016/j.rser.2016.06.082>.
- Bowman, Wesley. 2022. “UTide.” GitHub. <https://github.com/wesleybowman/Utide>.
- Cicilio, Phylcia, Jeremy VanderMeer, Steve Colt, Alexis Francisco, Emilia Sakai Hernandez, Cameron Morelli, Michelle Wilber, et al. 2024. *Alaska’s Railbelt Electric System: Decarbonization Scenarios for 2050*. Alaska Center for Energy and Power, University of Alaska, Fairbanks. UAF/ACEP/TP-01-0003. https://www.uaf.edu/acep/files/media/ACEP_Railbelt_Decarbonization_Study_Final_Report.pdf
- DeMarban, Alex. 2022. “Hilcorp Warns Alaska Utilities About Uncertain Cook Inlet Natural Gas Supplies.” *Anchorage Daily News*. Accessed May 19, 2023. <https://www.adn.com/business-economy/energy/2022/05/17/hilcorp-warns-alaska-utilities-about-uncertain-cook-inlet-natural-gas-supplies/>.
- Denholm, Paul, Marty Schwarz, and Lauren Streitmatter. 2024. *Achieving an 80% Renewable Portfolio in Alaska’s Railbelt: Cost Analysis*. Golden, CO: National Renewable Energy Laboratory. NREL/TP-6A40-85879. <https://www.nrel.gov/docs/fy24osti/85879.pdf>.
- Denholm, Paul, Marty Schwarz, Elise DeGeorge, Sherry Stout, and Nathan Wiltse. 2022. *Renewable Portfolio Standard Assessment for Alaska’s Railbelt*. Golden, CO: National Renewable Energy Laboratory. NREL/TP-5700-81698. <https://www.nrel.gov/docs/fy22osti/81698.pdf>.
- Homer Electric Association Inc. 2020. “2020 Annual Report.” https://www.homerelectric.com/wp-content/uploads/HEA-Ann-rpt-2020_printable.pdf.
- Homer Electric Association Inc. No date. “Bradley Lake Hydroelectric Plant.” Accessed May 25, 2023. <https://www.homerelectric.com/my-cooperative/power-generation/bradley-lake-project/>.
- Howell, David, and Eric Sandberg. 2022. “Alaska Population Projections: 2021 to 2050.” Juneau, AK: Alaska Department of Labor and Workforce Development. <https://live.laborstats.alaska.gov/pop/projections/pub/popproj.pdf>.
- International Electrotechnical Commission (IEC). 2015. “IEC TS 62600-101:2015 “Marine energy – Wave, tidal and other water current converters – Part 101: Wave energy resource assessment and characterization.” <https://webstore.iec.ch/publication/22593>.
- Kilcher, Levi, and James McVey. 2021. “2021 Cook Inlet Tidal Energy Resource Characterization Bottom Lander Measurements.” <https://dx.doi.org/10.15473/1876584>.

Kilcher, Levi, Michelle Fogarty, and Michael Lawson. 2021. *Marine Energy in the United States: An Overview of Opportunities*. Golden, CO: National Renewable Energy Laboratory. NREL/TP-5700-78773. <https://www.nrel.gov/docs/fy21osti/78773.pdf>.

Klima, Kelly, and Jay Apt. 2015. “Geographic Smoothing of Solar PV: Results from Gujarat.” *Environmental Research Letters* 10: 104001. DOI 10.1088/1748-9326/10/10/104001.

Lew, D., G. Brinkman, E. Ibanez, A. Florita, M. Heaney, B.-M. Hodge, M. Hummon, et al. 2013. *The Western Wind and Solar Integration Study Phase 2*. Golden, CO: National Renewable Energy Laboratory. NREL/TP-5500-55588. <https://www.nrel.gov/docs/fy13osti/55588.pdf>.

Lewis, Matt, Rory O’Hara Murray, Sam Fredriksson, John Maskell, Anton de Fockert, Simon P. Neill, and Peter E. Robins. 2021. “A Standardized Tidal-Stream Power Curve, Optimised for the Global Resource.” *Renewable Energy* 170: 1308–1323. <https://doi.org/10.1016/j.renene.2021.02.032>.

Marohl, Brett. 2021. “Oil Production in Alaska Reaches Lowest Level in More Than 40 Years.” U.S. Energy Information Administration, Today in Energy. Accessed May 19, 2023. <https://www.eia.gov/todayinenergy/detail.php?id=47696>.

Musial, Walt, Donna Heimiller, Philipp Beiter, George Scott, and Caroline Draxl. 2016. *2016 Offshore Wind Energy Resource Assessment for the United States*. Golden, CO: National Renewable Energy Laboratory. NREL/TP-5000-66599. <https://www.nrel.gov/docs/fy16osti/66599.pdf>.

National Oceanic and Atmospheric Administration (NOAA). 2023. “Current Meter Stations.” C-MIST. <https://cmist.noaa.gov/cmist/ssl/welcome.do>.

Rodrigue, Jean-Paul. 2020. *The Geography of Transport Systems*. New York: Routledge. <https://doi.org/10.4324/9780429346323>.

Stanley, Andrew P. J., Owen Roberts, Anthony Lopez, Travis Williams, and Aaron Barker. 2022. “Turbine Scale and Siting Considerations in Wind Plant Layout Optimization and Implications for Capacity Density.” *Energy Reports* 8: 3507–3525. <https://doi.org/10.1016/j.egy.2022.02.226>.

U.S. Energy Information Administration. 2023. “Alaska State Energy Profile.” Accessed May 25, 2023. <https://www.eia.gov/state/print.php?sid=AK>.

U.S. Environmental Protection Agency (EPA). 2023. “Emissions & Generation Resource Integrated Database (eGRID).” <https://www.epa.gov/egrid>.

Appendix A. Device and Array Sizing

The annual energy production (AEP) of the array can be computed via different yet equivalent equations per International Electrotechnical Commission (IEC) Technical Standard 62600-101:2015 (IEC 2015):

$$AEP = \overline{N^*}(1 - \beta) \sum_{U_{\text{bins}}} P(U) \cdot H(U) = \Delta t \sum_{1\text{-year}} \mathcal{P}_{\text{array}}(U(t), t) \quad (\text{A-1})$$

Here, $H(U)$ is the amount of time in a year (a histogram) that the site has an inflow speed that falls within each speed bin, and U_{bins} is the set of inflow speed bins that span the inflow speeds observed at the site. $\overline{N^*}$ is the time-averaged availability of devices within the array. In this approach, U is the speed at the center of the bin, and we use speed bins that are spaced 0.1 m/s apart. In the second approach, we use a time-step spacing (Δt) equal to 5 minutes. To improve the accuracy of the AEP estimate, we use the tidal harmonic fits—to the measured data—to extrapolate the measurements to a full year. We then estimate the capacity factor according to:

$$CF = \frac{AEP_{\text{array}}}{N \cdot P_{\text{rated}} \cdot (1\text{-year})} \quad (\text{A-2})$$

Sizing the device for each site starts by identifying the size of the rotor that can reasonably fit in the water column. In this work, we assume that container ships will need to be able to pass over the tidal array without risk of collision, and that the bottom of the rotor will need to be at least 5 m above the seafloor. At present, the largest container ships have a draft less than 18 m (Rodrigue 2020). At the East Foreland site, for example, the channel has a maximum depth of approximately 60 m and is more than 43 m deep over a large area. Therefore, a turbine with $d_{\text{rotor}} = 20$ m could be deployed in this channel without interfering with vessel traffic ($d_{\text{rotor}} + D_{\text{draft}} + h_{\text{bottom}} = 20 \text{ m} + 18 \text{ m} + 5 \text{ m} = 43 \text{ m}$).

There is an inherent trade-off between increasing project cost by increasing the size of the generator (and increasing transmission capacity to match) versus maximizing power production. To size the device generator for each site, we calculate a single-device AEP (AEP_1) and capacity factor (CF_1) by letting $N^* = N = 1$ and $\beta = 0$. For example, a generator size $P_{\text{rated}} = 0.6$ MW (Figure A-1) deployed at the East Foreland site (with $d_{\text{rotor}} = 20$ m) will produce $AEP_1 = 2,695$ MWh/yr and have a capacity factor $CF_1 = 51\%$. A device rated to be nearly twice as big ($P_{\text{rated}} = 1.17$ MW) will produce an additional 769 MWh/yr (3,464 MWh/yr total) and have a capacity factor of 34%. Further increasing the generator size to 1.7 MW will generate an additional 146 MWh/yr (3,610 MWh/yr total) and have a capacity factor of 24%, as shown in Figure A-1. This indicates the diminishing returns on increasing generator capacity.

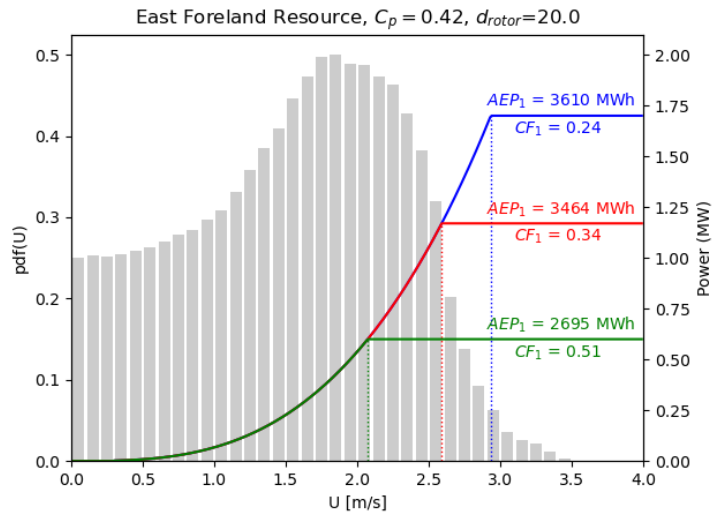


Figure A-1. The generator power curve (right axis), and probability density function (pdf) of ocean velocity at the East Foreland (bars, left axis). The power curve is plotted for three different generator sizes, with three different capacity factors.

Rather than sizing the generator based on economics—because cost is beyond the scope of this work—we size the generator to capture 95% of the maximum energy available at the site with the selected turbine. In the case of the resource at the East Foreland site (Figure A-2), for a turbine with $d_{rotor} = 20$ m and $C_p = 42\%$, 95% of the energy can be captured with the 1.17-MW generator. As discussed above (the red power curve in Figure A-1), this will generate 3,464 MWh/yr, have a $CF_{1@95\%} = 34\%$, and have a $U_{rated@95\%} = 2.59$ m/s.

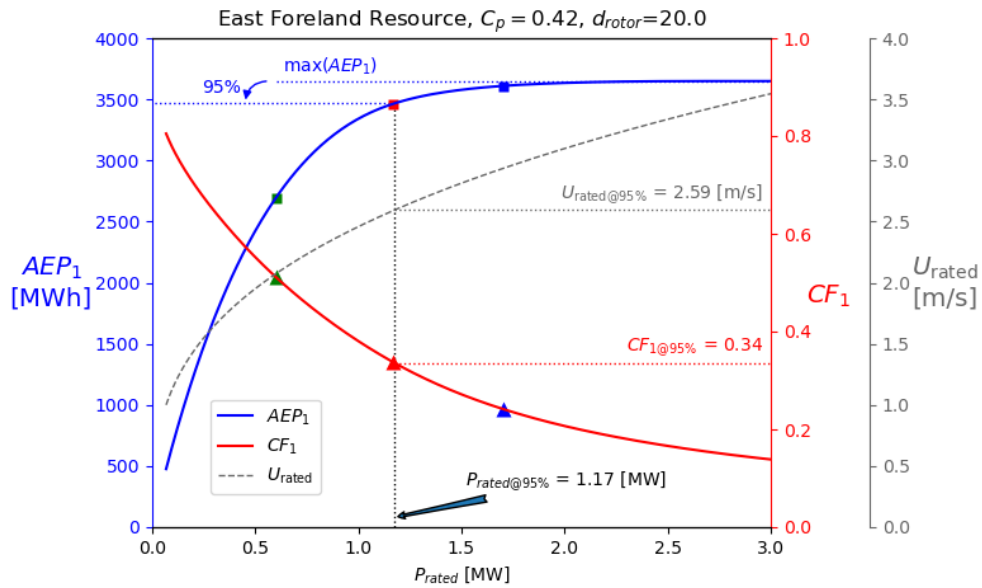


Figure A-2. Total power captured at the East Foreland site for a single device (left, blue axis), the capacity factor for the device (right, red axis), and U_{rated} versus generator capacity (P_{rated}). The square and triangle markers indicate the AEP and capacity factor, respectively, for the generator sizes in Figure A-1. Dotted lines indicate the values for sizing the generator to capture 95% of the power available to the rotor. In this case, 95% of the maximum AEP can be captured with a 1.17-MW generator.

This approach to device sizing is repeated for the other sites we consider (Kennedy Entrance, Anchor Point, and Fire Island), and the results are shown in Table 2. We also estimate the number of turbines required for an array with 100 MW of capacity. To estimate the spatial dimensions of these arrays, we follow best practices of the wind industry and assume that turbines are spaced $10 \cdot d_{rotor}$ in the streamwise direction $3 \cdot d_{rotor}$ across the channel (Figure A-3). With these assumptions the array width is $W = 3 \cdot d_{rotor} \cdot (N_{cols} - 1) + d_{rotor}$, and the length is $L = 10 \cdot d_{rotor} \cdot (N_{rows} - 1)$. We then assume that the arrays will be approximately twice as wide as they are long to get a final estimate of the array dimensions (Figure A-3).

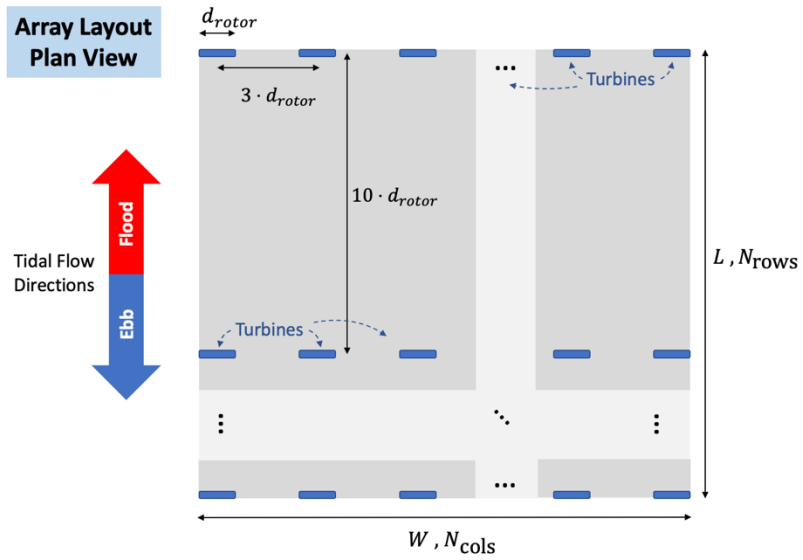


Figure A-3. Array layout diagram in plan view (i.e., from above looking down)

Appendix B. Full Set of Generation Results

Figure B-1 and Figure B-2 plot the annual total generation stacks for all scenarios studied, aggregated by technology, for the entire Railbelt. The latter figure plots the total generation stacks less the Basecase stack, which includes no tidal energy. These plots are equivalent to Figure 4 and Figure 5, respectively, in the main body of the text; except those plots removed the intermediate tidal energy capacities (150, 175, 200, 300, and 400 MW) for clarity. The plots presented here better highlight the impact of gradually increasing tidal capacity for a given infrastructure scenario.

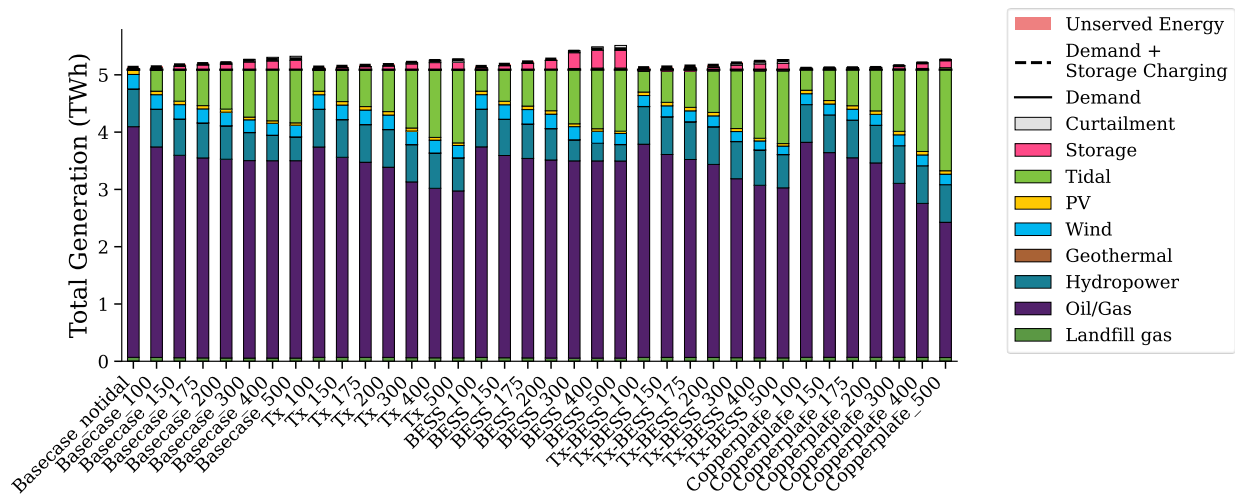


Figure B-1. Total generation stacks for all scenarios studied. Results plotted are Railbelt-wide.

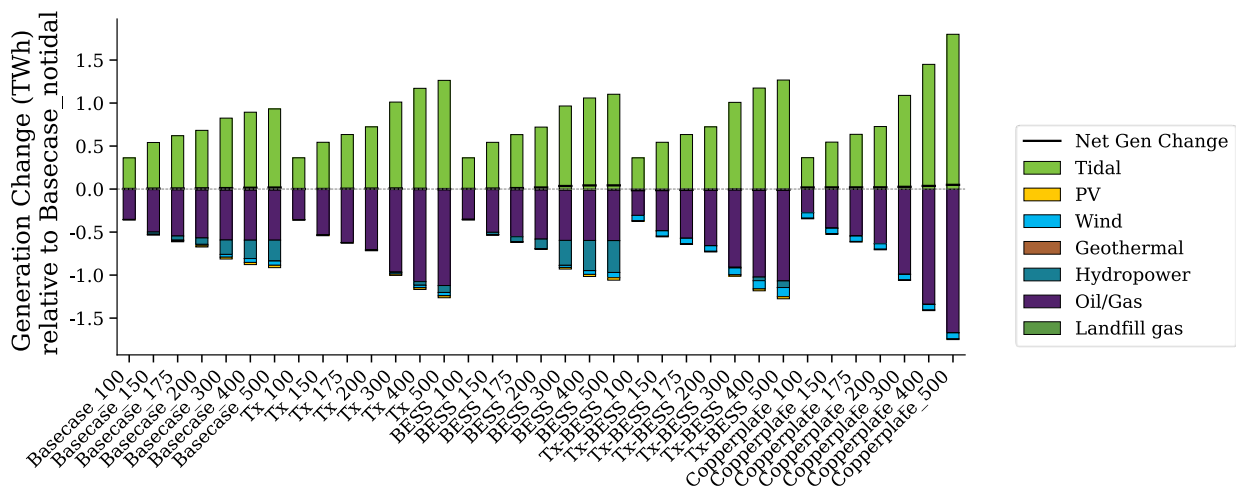


Figure B-2. Total generation stacks, differenced from the Basecase with no tidal energy, for all scenarios studied. Results plotted are Railbelt-wide.